Molecular Imaging: Reporter Gene Imaging

Inna Serganova, Phillipp Mayer-Kukuck, Ruimin Huang, and Ronald Blasberg(✉)

Abstract Non-invasive in-vivo molecular genetic imaging developed over the past decade and predominantly utilises radiotracer (PET, gamma camera, autoradiography), magnetic resonance and optical imaging technology. Molecular genetic imaging has its roots in both molecular biology and cell biology. The convergence of these disciplines and imaging modalities has provided the opportunity to address new research questions, including oncogenesis, tumour maintenance and progression, as well as responses to molecular-targeted therapy. Three different imaging strategies are described: (1) "bio-marker" or "surrogate" imaging; (2) "direct" imaging of specific molecules and pathway activity; (3) "indirect" reporter gene imaging. Examples of each imaging strategy are presented and discussed. Several applications of PET- and optical-based reporter imaging are demonstrated, including signal transduction pathway monitoring, oncogenesis in genetic mouse models, endogenous molecular genetic/biological processes and the response to therapy in

Ronald Blasberg
Departments of Neurology and Radiology, Memorial Sloan-Kettering Cancer Center, 1275 York Avenue, New York, NY 10021, USA
blasberg@neuro1.mskcc.org

W. Semmler and M. Schwaiger (eds.), *Molecular Imaging II.*
Handbook of Experimental Pharmacology 185/II.

animal models of human disease. Molecular imaging studies will compliment established ex-vivo molecular-biological assays that require tissue sampling by providing a spatial and a temporal dimension to our understanding of disease development and progression, as well as response to treatment. Although molecular imaging studies are currently being performed primarily in experimental animals, we optimistically expect they will be translated to human subjects with cancer and other diseases in the near future.

1 Introduction

Medical imaging has undergone a remarkable revolution and expansion in the past two decades, and this expansion coincides with novel molecular-based medical therapies that have emerged following the complete sequencing of the human genome. Recent progress in our understanding of the molecular genetic mechanisms in many diseases and the application of new biologically based approaches in therapy are exciting new developments. Novel "molecular therapies" have been developed that target specific oncogenic mutations in chronic myelogenous leukemia (CML) (Druker et al. 1996), gastrointestinal stromal tumours (GIST) (Tuveson et al. 2001), and lung cancer (Lynch et al. 2004). New gene-based therapies can provide control over the level, timing and duration of action of many biologically active transgene products by including specific promoter/activator regulatory elements in the genetic material that is transferred. Controlled gene delivery and gene expression systems have recently been developed for specific somatic tissues and tumours (Papadakis et al. 2004; Ray et al. 2004; Zhu et al. 2004; Sadeghi and Hitt 2005). For example, novel gene constructs that target vectors to specific tissues/organs, and for controlling gene expression using cell-specific, replication-activated and drug-controlled expression systems. In addition, small radiolabelled compounds and paramagnetic probes are being developed to image specific proteins in specific signalling cascades, and they are being applied to monitor drug response. The inclusion of non-invasive imaging of specific molecular genetic and cellular processes will accelerate our research efforts and lead to more effective therapeutic strategies (Harrington et al. 2000; Nakagawa et al. 2001).

Molecular imaging provides visualisation in space and time of normal as well as abnormal cellular processes at a molecular genetic or cellular level of function. Although the term "molecular imaging" was coined in the mid 1990s, it has its roots in molecular biology and cell biology, as well as in imaging technology and chemistry. For example, for many years researchers used reporter genes encoding enzymes, such as bacterial β-galactosidase (*lacZ* gene) (Forss-Petter et al. 1990) and chloramphenicol acetyltransferase (*CAT* gene) (Overbeek et al. 1985), to study various cellular processes. However, 'visualisation' of these enzymes required post-mortem tissue sampling and processing for precise quantitative analysis. Advances in cell biology, especially the translation of these advances to clinical applications, dictate the development of novel visualisation systems that would provide accurate

and sensitive measurements, as well as allow visualisation in living cells, live animals and human subjects.

Molecular imaging in living animals is the direct result of significant developments in several non-invasive, in-vivo imaging technologies: (1) magnetic resonance (MR) imaging (Ichikawa et al. 2002); (2) nuclear imaging (QAR, gamma camera and PET) (Blasberg and Gelovani 2002); (3) optical imaging of small animals (Edinger et al. 2002; Weissleder 2002; Hoffman 2005), as well as two-photon fluorescent imaging of viable cells, small organisms and embryos (Hadjantonakis et al. 2002). It should be noted that these developments occurred more or less in parallel to each other, and were largely independent of the advances that were occurring in genetics and in molecular and cell biology during the 1980s and early 1990s. However, each of these imaging technologies have had important antecedents. For example, radionuclide-based imaging is founded on the radiotracer principle, first described by George de Hevesy. In 1935, he published a letter in *Nature* on the tracer principle using ^{32}P for the study of phosphorus metabolism (Chievitz and Hevesy 1935; Myers 1979) and he was awarded the Nobel Prize in Chemistry in 1943. The tracer technique was later adapted for many applications in physiology and biochemistry, as well as in functional diagnosis and use in nuclear medicine and molecular imaging.

The convergence of the imaging and molecular/cell biology disciplines in the mid 1990s is at the heart of this success story and it is the wellspring for further advances in this new field. Although first applied to non-invasive in-vivo imaging of small animals, molecular imaging paradigms are now being translated into clinic imaging paradigms (Jacobs et al. 2001b; Penuelas et al. 2005) that will establish new standards of medical practice. The development of versatile and sensitive non-invasive assays that do *not* require tissue samples will be of considerable value for monitoring molecular-genetic and cellular processes in animal models of human disease, as well as for studies in human subjects in the future.

This new field of investigation has expanded rapidly following the establishment of “cancer imaging” as one of six “extraordinary scientific opportunities” by NCI in 1997-98. Subsequent funding initiatives have provided a major stimulus to further the development of this new discipline. Substantial resources have been made available to the research community through NCI’s Small Animal Imaging Resources Program (SAIRP) and the In Vivo Cellular and Molecular Imaging Centers (ICMIC) program. Similar funding initiatives have been developed by other NIH Institutes and by the Department of Energy (DOE). In addition, a new NIH institute — the National Institute for Biomedical Imaging and Bioengineering (NIBIB) — has recently been formed to better represent the breadth of an expanding imaging community. In addition, there are two new journals devoted the field of molecular imaging — Molecular Imaging (BC Decker, Publisher; the official journal of the Society of Molecular Imaging, www.molecularimaging.org) and Molecular Imaging and Biology (Springer New York, Publisher; the official journal of the Academy of Molecular Imaging, www.ami-imaging.org), and other established imaging-related journals have added “molecular imaging” components.

2 Molecular Imaging Strategies

The most widely used molecular imaging modalities include: (1) optical (fluorescence, bioluminescence, spectroscopy, optical coherence tomography), (2) radionuclide (PET, SPECT, gamma camera, autoradiography) and (3) magnetic resonance (spectroscopy, contrast, diffusion-weighted imaging). In addition, other modalities, such as ultrasound and CT, are seeing increasing application and could be included as well. The interaction of several disciplines, including molecular cell biology and chemistry with different imaging modalities is illustrated by the Ven diagram (Fig. 1), and illustrates the theme of this presentation. Namely, a multi-modality, multi-disciplinary approach to molecular imaging provides many positive advantages. Several of the imaging modalities (fluorescence, bioluminescence, nuclear, and magnetic resonance) are illustrated in the following sections and their combined advantage are highlighted.

Before discussing specific molecular imaging issues, it would be helpful to briefly outline three currently used imaging strategies to non-invasively monitor and measure molecular events. They have been broadly defined as "biomarker", "direct" and "indirect" imaging. These strategies have been discussed previously in several recent reviews (Contag et al. 1998; Gambhir et al. 2000b; Tavitian 2000; Berger and Gambhir 2001; Ray et al. 2001; Blasberg and Gelovani 2002; Gelovani Tjuvajev and Blasberg 2003; Luker et al. 2003c; Weissleder and Ntziachristos 2003) and in other perspectives on molecular imaging (Blasberg and Gelovani 2002; Contag and Ross 2002; Gambhir 2002; Weissleder and Ntziachristos 2003; Min and Gambhir 2004; Shah et al. 2004).

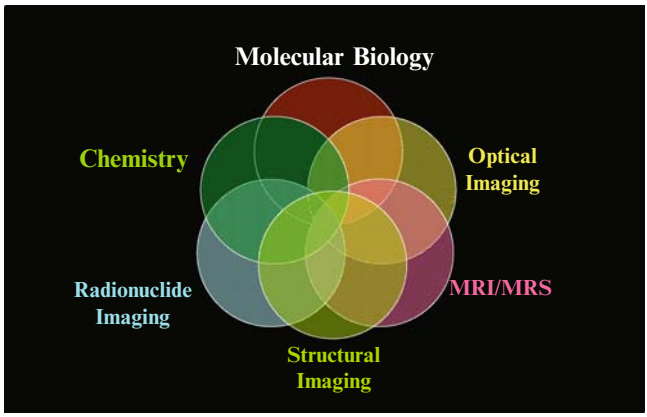

Fig. 1 Multidisciplinary approach to molecular imaging. Molecular and cell biology, along with chemistry, provide the foundation and resources for developing novel in-vivo molecular constructs and imaging paradigms. Three imaging modalities currently dominate the field, along with structural/anatomical imaging. This list will likely expand to include other modalities in the near future. The *Ven diagram* emphasizes the interaction between disciplines and different imaging modalities; it is this interaction that provides a broad new approach to the field

2.1 Biomarker Imaging

Biomarker or surrogate-marker imaging can be used to assess downstream effects of one or more endogenous molecular genetic processes. This approach is particularly attractive for potential translation into clinical studies in the short-term, because existing radiopharmaceuticals and imaging paradigms may be useful for monitoring downstream effects of changes in specific molecular genetic pathways in diseases such as cancer. For example, tumour imaging of glucose utilisation using a radiolabelled analogue of glucose (2′-fluoro-2′-deoxyglucose — [^{18}F]FDG) and positron emission tomography (PET) is based on the fact that malignant tumours frequently have high glycolytic rates (Warburg 1956). The images of increased glucose utilisation and increased glycolysis reflect increased glucose transport and hexokinase activity, as well as the pathways that regulate these processes. This imaging strategy has been recognized for nearly three decades and was initially applied to malignant brain tumours by Di Chiro et al. (1982). Only small-bore (head-only) PET tomographs were available at that time, until the introduction of commercial whole-body PET scanners in the early 1990s. Now, whole-body [^{18}F]FDG PET imaging is routinely and widely used in the clinic for tumour diagnosis and staging the extent of disease (Shreve et al. 1999), as well as for monitoring the efficacy of anti-cancer therapies (Schelling et al. 2000).

The regulation of glucose utilisation in cells is complex and reflects the sum of multiple inputs at various levels involving different signalling pathways. For example, increased glycolysis can be a response to an increase in cellular energy and substrate requirements, to an increase in cell proliferation and synthesis rates, and to the activation of specific oncogenic pathways that can occur in the presence of adequate oxygen (Warburg effect). Although glucose uptake and glycolytic enzyme activity are homeostatically regulated, glucose metabolism has also been shown to be regulated by extracellular signals mediated by cell surface receptors such as cKIT. Receptor-mediated regulation of glucose uptake is thought to involve activation of PI3 kinase, Akt, mTOR (the kinase mammalian target of rapamycin) and S6 kinase. Examples of this include the CD28 signalling pathway in T-cells and insulin receptor signalling (Frauwirth et al. 2002). A likely explanation for the dramatic effect of STI571 (Gleevec) on glucose uptake in GIST is that c-Kit receptor signalling regulates/mediates glucose uptake as well as glucose metabolism. Interestingly, in a lymphoma and a lymphocyte cell line, mTOR depletion or rapamycin treatment and glucose deprivation trigger a stress response similar to a starvation phenotype (Peng et al. 2002). In addition, various inputs that increase HIF-1α levels impact on and increase glycolysis through enhanced translation and transcription; similarly, the mutation and functional inactivation of specific proteins (e.g. VHL and p53) that results in stabilisation and reduced degradation rate of the HIF-1α protein also increase glucose transport and glycolysis.

Biomarker [^{18}F]FDG PET studies have been extensively used to assess biological effects occurring during neoplastic progression and to monitor the effects of therapy. However, biomarker imaging may be relatively “non-specific”, in that it is likely to reflect effects on more than a single protein or signalling pathway. Nevertheless,

it benefits from the use of radiolabelled probes that have already been developed and studied in human subjects. Thus, the translation of biomarker imaging paradigms into patients will be far easier than either the direct imaging paradigms or reporter transgene imaging paradigms outlined below. However, it remains to be shown whether there is a sufficiently high correlation between "surrogate marker" imaging and direct molecular assays that reflect the activity of a particular molecular/genetic pathway of interest.

Very few studies have attempted a rigorous correlation between biomarker imaging and transcriptional activity of a particular gene, or post-transcriptional processing of the gene product, or the activity of a specific signal transduction pathway that is targeted by a particular drug. The application of biomarker imaging for monitoring treatment response is gaining increasing attention, particularly as it relates to the development and testing of new pathway-specific drugs. One recent example of clinically useful biomarker imaging is the early (1–7 days) assessment of treatment response with [^{18}F]FDG PET imaging, as applied to gastrointestinal stromal tumours (GIST) pre- and post-imatinib mesylate (Gleevec, Glivec, STI571) treatment (Demetri et al. 2002) (Fig. 2a). This is significant because imatinib mesylate treatment specifically targets the c-Kit receptor tyrosine kinase that is mutated and constitutively over-expressed in GIST, and the metabolic response to treatment is observed within hours. [^{18}F]FDG PET imaging is also useful in monitoring patients with GIST for recurrent disease or failure of current therapy (Fig. 2b).

Several clinical cancer trials involving mTOR inhibitors have been shown sporadic anti-tumour activity, leading to uncertainty about the appropriate clinical setting for their use. Recently Thomas et al. (2006) have shown that loss of the Von Hippel-Lindau tumour suppressor gene (VHL) sensitizes kidney cancer cells to the mTOR inhibitor CCI-779, both in vitro and in mouse tumour models. Growth arrest caused by CCI-779 was shown to correlate with a block in translation of mRNA encoding the hypoxia-inducible factor (HIF-1α), and VHL-deficient tumours showed increased uptake of [^{18}F]FDG in an mTOR-dependent manner. Prior clinical PET studies in individuals with kidney cancer indicate that only a proportion ($\sim$50–70%) of these tumours accumulate FDG to high levels, consistent with the expected frequency of VHL loss (Hain and Maisey 2003). These findings provide preclinical data for prospective, [^{18}F]FDG PET biomarker-driven clinical studies of mTOR inhibitors in kidney cancer. It suggests that [^{18}F]FDG PET scans could be used as a pharmacodynamic marker of treatment potential as well as response. Whether imaging "surrogate markers" will be of value for assessing treatment directed at other molecular/genetic abnormalities in tumours (EGFR, p53, c-Met, HIF-1, etc.) remains to be demonstrated.

PET with [^{18}F]FDG is approved by the Center for Medicare and Medicaid Services in the United States for diagnosing, staging, and restaging lung cancer, colorectal cancer, lymphoma, melanoma, head and neck cancer, and esophageal cancer. Unfortunately, tumour cells are not the only cells that have high uptake of [^{18}F]FDG. Recently, Maschauer and co-workers have shown that endothelial cells within the tumours and vascular lesions exhibit high [^{18}F]FDG uptake, and that it correlates with enhanced by vascular endothelial growth factor (VEGF) expression. VEGF

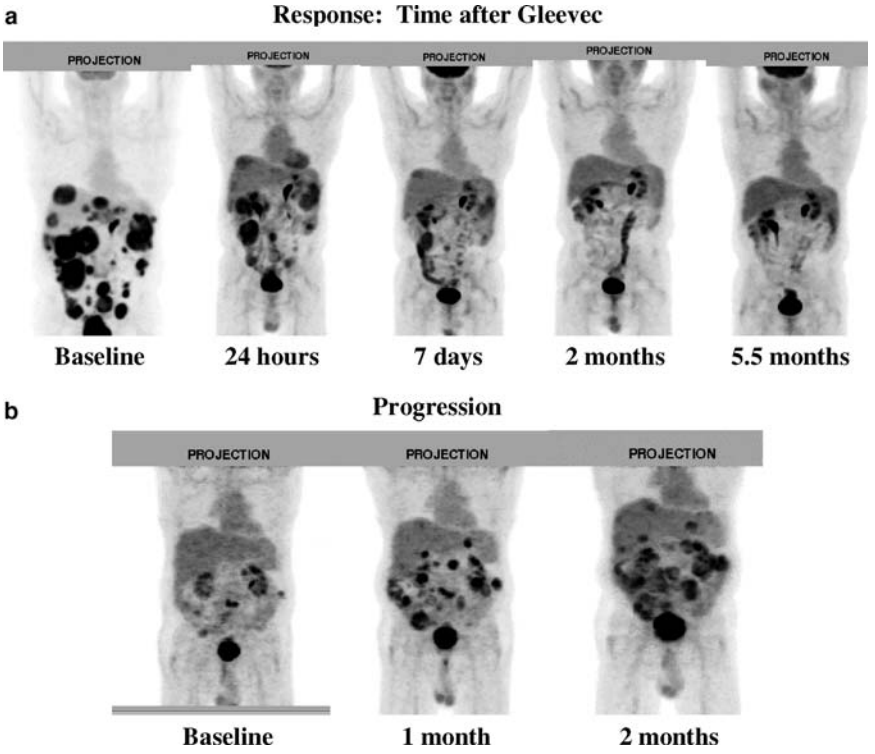

Fig. 2 [^{18}F]FDG PET imaging of GIST before and after treatment. In patients with gastrointestinal stromal tumours (GIST), tumour glucose utilisation is very high and these tumours can be readily visualised by [^{18}F]FDG PET. A striking observation in patients with GIST who are treated with STI571 (Gleevec) was the rapid and a decrease in [^{18}F]FDG uptake determined by PET scan was seen as early as 24 h after one dose of STI571, and this was sustained over many months **a**. Correspondingly, treatment failure and progression of disease can be readily monitored by [^{18}F]FDG PET **b**. The high FDG levels seen in the kidney, ureter and bladder are normal in both the pre- and post-Gleevec images. [Adapted from van den Abbeele (2001), with appreciation and permission from Dr. Annick Van den Abbeele, Dana-Farber Cancer Institute, Boston, Massachusetts]

stimulates the proliferation and migration of vascularly derived endothelial cells and it is highly expressed in a variety of tumours, including renal, breast, ovary, and colon cancer (Maschauer et al. 2004). Numerous reports have shown that lesions with a high concentration of inflammatory cells, such as neutrophils and activated macrophages, also show increased [^{18}F]FDG uptake, which can be mistaken for malignancy in patients with proven or suspected cancer (Brown et al. 1996).

[^{18}F]FDG PET has been repeatedly shown to improve staging accuracy compared with CT scanning alone, and it provides a cost-effective adjunct to the preoperative staging of NSCLC and lung metastases (Hoekstra et al. 2003). Combined [^{18}F]FDG PET-CT imaging has been shown to be effective in demonstrating early (at 3 weeks) response (Fig. 3a) as well as failure to chemotherapy (Fig. 3b). However, in patients with adenocarcinoma and mediastinal lymph nodes of < 1 cm,

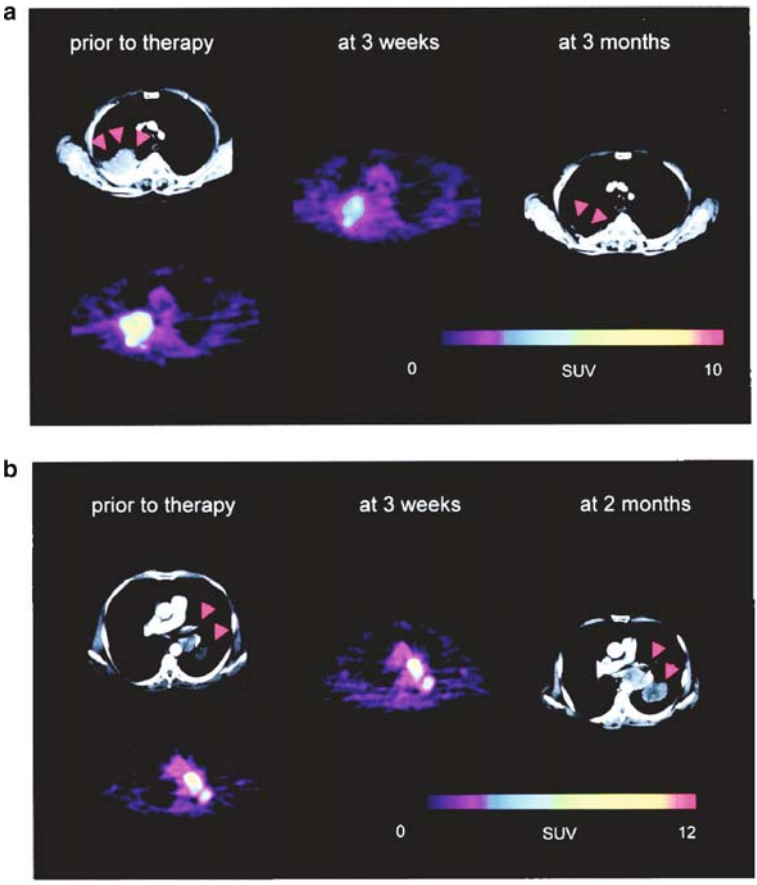

Fig. 3 [^{18}F]FDG PET imaging lung tumours before and after treatment. [^{18}F]FDG PET and CT scans of two patients with lung tumours: a responding patient **a** and a non-responding patient **b**. In the responding tumour, there is a 61% decrease in FDG uptake 3 weeks after initiation of chemotherapy. In contrast, tumour FDG uptake is essentially unchanged in the non-responding tumour. (Adapted from Weber et al. 2003)

[^{18}F]FDG PET scanning cannot yet replace mediastinoscopy (Kelly et al. 2004). This imaging modality is also having an impact on radiation therapy volume delineation in NSCLC. Radiation targeting based on fused [^{18}F]FDG PET and CT images resulted in alterations in radiation therapy planning in over 50% of patients by comparison with CT targeting (Bradley et al. 2004). [^{18}F]FDG PET is also being used to assess response to chemotherapy and may have predictive value. A reduction in metabolic activity after one cycle of chemotherapy has been shown to be correlated with final outcome of therapy (Weber et al. 2003). The use of metabolic markers to determine response may shorten the duration of phase II studies evaluating new cytotoxic drugs, and may decrease the morbidity and costs of therapy in non-responding patients.

2.2 Direct Molecular Imaging

Direct imaging strategies are usually described in terms of a specific target and a target-specific probe. This strategy has been established using nuclear, optical and MR imaging technology. The resultant image of probe localisation and concentration (signal intensity) is directly related to its interaction with the target. Imaging cell-surface-specific antigens with radiolabelled antibodies and genetically engineered antibody fragments, such as *minibodies*, are examples of direct molecular imaging that have evolved over the past 30 years. In addition, in-vivo imaging of receptor density/occupancy using small radiolabelled ligands has also been widely used, particularly in neuroscience research, over the past two decades. These examples represent some of the first molecular imaging applications used in clinical nuclear medicine research. More recent research has focused on chemistry and the synthesis of small radiolabelled or fluorescent molecules (and paramagnetic nanoparticles) that target-specific receptors (e.g. the estrogen or androgen receptors) (Dehdashti et al. 1995; Larson et al. 2004) and fluorescent probes that are activated by endogenous proteases (Jaffer et al. 2002). For example, the alpha(v)beta3 integrin is highly expressed on tumour vasculature and plays an important role in metastasis and tumour-induced angiogenesis; initial studies of targeting and imaging of the alpha(v)beta3 integrin with radiolabelled glycosylated RGD-containing peptides are very encouraging (Fig. 4) (Halbhuber and Konig 2003). Another example is direct imaging of the cell-surface-receptor tyrosine kinase HER2, which is over-expressed in many breast tumours. The level of expression of HER2 can be imaged with radiolabelled (Blend et al. 2003; Palm et al. 2003; Funovics et al. 2004) or gadolinium-chelated (Artemov et al. 2003) antibodies specific for HER2.

Other direct radiotracer imaging strategies involve the development of radiolabelled antisense and aptomer oligonucleotide probes (RASONs) that specifically hybridize to target mRNA. Some efficacy for gamma camera and PET imaging endogenous gene expression using RASONs has been reported (Dewanjee et al. 1994; Cammilleri et al. 1996; Phillips et al. 1997; Tavitian et al. 1998). Nevertheless, RASON imaging has several serious limitations, including: (1) low number of target mRNA/DNA molecules per cell; (2) limited tracer delivery (poor cell membrane, vascular and blood-brain barrier permeability); (3) poor stability; (4) slow clearance of non-bound oligonucleotides); (5) comparatively high background activity and low specificity of localisation (low target/background ratios). A further constraint limiting direct radiotracer imaging strategies is the necessity to develop a specific probe for each molecular target, and then to validate the sensitivity, specificity and safety of each probe for specific applications. This can be very time consuming and costly. For example the development, validation and regulatory approval for [^{18}F]FDG PET imaging of glucose utilisation in tumours has taken over 20 years.

The diagnostic potential of radiolabelled antibodies that localise specifically to tumours has been incrementally developed over three decades. Currently available antibodies (and large antibody fragments) suffer several drawbacks as radiolabelled pharmaceuticals. This is primarily related to the prolonged biological half-life of intact antibodies, leading to high background signal. A promising approach has been

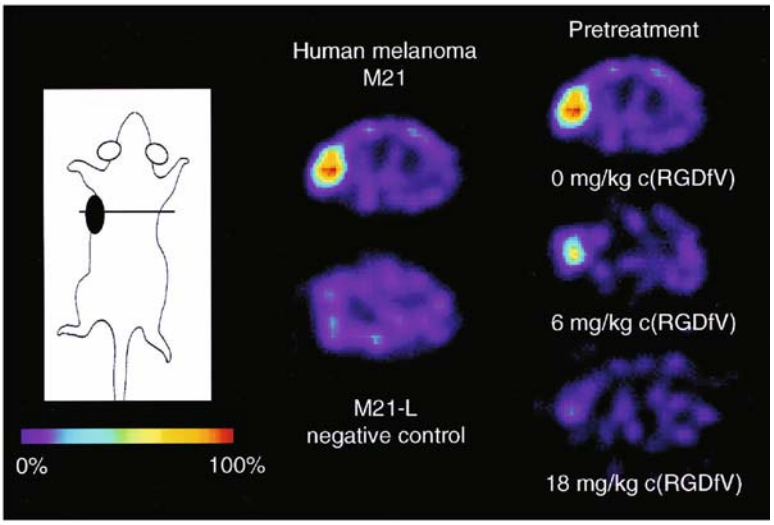

Fig. 4 Non-invasive imaging of alpha(v)beta(3) integrin expression by PET. Transaxial PET images of nude mice bearing human melanoma xenografts. Images were acquired 90 min after injection of approximately 5.5 MBq of [^{18}F]Galacto-RGD. The *top left* image shows selective accumulation of the tracer in the alpha(v)beta(3)-positve $(M21)$ tumour on the left flank. No focal tracer accumulation is visible in the alpha(v)beta(3)-negative $(M21-L)$ control tumour (*bottom left image*). The three images on the *right* were obtained from serial [^{18}F]Galacto-RGD PET studies in one mouse. These images illustrate the dose-dependent blockade of tracer uptake by the alpha(v)beta(3)-selective cyclic pentapeptide cyclo (-Arg-Gly-Asp-D-Phe-Val-). (Adapted from Haubner et al. 2001)

to genetically engineer small radiolabelled antibody fragments to have high targeted localisation to a specific antigen, with low non-target binding and rapid clearance from the body. For example, a series of engineered antibody fragments was derived from the parental murine monoclonal antibody T84.66. These fragments were selected for high affinity and specificity for carcinoembryonic antigen (CEA), an antigen highly expressed in colorectal carcinoma and frequently elevated in adenocarcinomas of the lung, breast, other gastrointestinal organs, and ovary (Neumaier et al. 1990). An engineered fragment called the minibody (an scFv-C_H3 fusion protein) have been constructed, radiolabelled with $^{123}\mathrm{I}(t_{1/2} = 13\,\mathrm{h})$, and evaluated in vivo using a standard gamma camera (Wu 2004; Wu and Senter 2005). The evaluation of this minibody labelled with a positron-emitting radionuclide, copper-64 $(t_{1/2} = 6\,\mathrm{h})$, was performed soon after; as expected, liver activity was elevated and this limited imaging applications to extrahepatic sites. To overcome these obstacles, later work by the same group demonstrated that radiolabelling anti-CEA minibodies and diabodies with a longer-lived positron emitter, iodine-124 $(t_{1/2} = 4$ days), resulted in excellent tumour targeting and visualisation by PET imaging at later times (1–4 days). The high target-to-background achieved in the PET images was predominantly due to low background activity following clearance of radioactivity from normal tissues (Sundaresan et al. 2003) (Fig. 5).

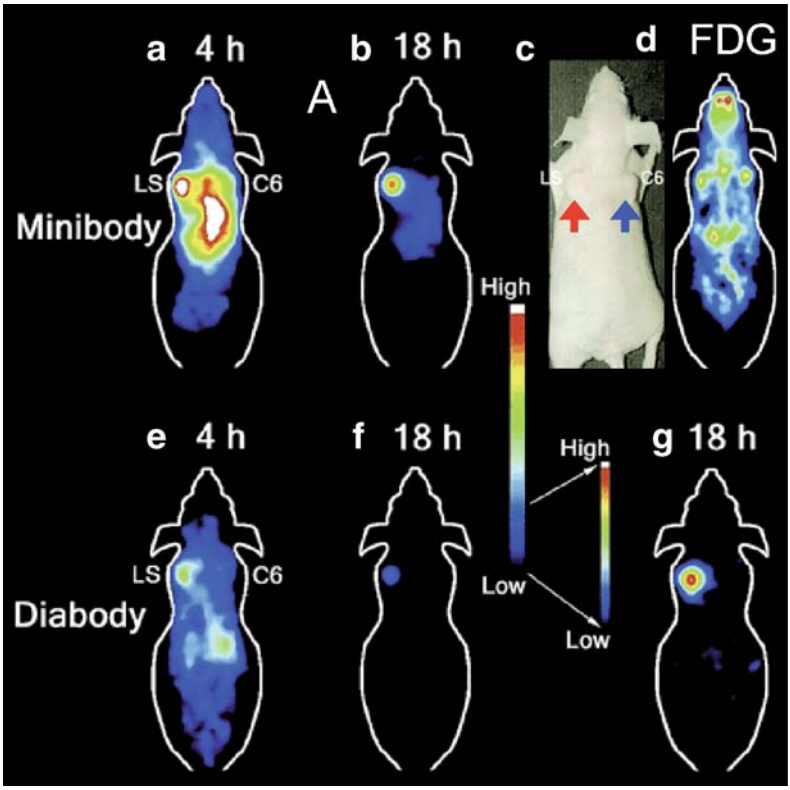

Fig. 5 Comparison of ^{124}I minibody and ^{124}I diabody by serial PET imaging. Mice bearing LS174T (LS, left shoulder) and C6 rat glioma (C6, right shoulder, negative control) xenografts were injected via tail vein with 1.9–3.1 MBq (65–85 µCi) ^{124}I minibody **a, b** or diabody **e, f** and imaged at 4 and 18 h. A photograph of the mouse with *arrows* pointing to the tumours **c** and an [^{18}F]FDG microPET scan **d** show the location of the xenografts. At 18 h, background activity in the animal was minimal compared with the 4-h images, resulting in high contrast. **a**, **b**, **e** and **f** are colour-coded to the same radioactivity scale. Image **f** was rescaled in **g** to illustrate the excellent contrast achieved with the ^{124}I diabody at 18 h. (Adapted from Sundaresan et al. 2003)

Another example of this approach is the development of anti-p185^{HER2} minibodies. These minibodies have high specific binding to p185^{HER2}-positive cells in vitro. One variant was radioiodinated and evaluated for its blood clearance, tumour-targeting properties, and normal organ uptake of the radiolabel in nude mice bearing p185^{HER2}-positive xenografts. The anti-p185^{HER2} 10H8 minibody showed the expected blood clearance, but the tumour activity reached a maximum of only $5.6 \pm 1.7\%$ ID/g at 12 h. Tumour localisation and persistance was substantially less than that previously observed with the radioiodinated anti-CEA minibody, and illustrates the variability in the kinetics of minibody targeting and biodistribution in different tumours. These differences were thought to be partially due to some combination of internalization, metabolism and dehalogenation of the minibody fragment (Olafsen et al. 2005).

Recent developments in MR imaging have enabled direct in-vivo imaging at high resolution ($\sim$50 µm) (Johnson 1993; Jacobs 1999). This approach is largely based on labelling cells with superparamagnetic iron oxide (SPIO) particles that permit visualisation and tracking of cells using MRI based on the large susceptibility artefacts (T_2^*-effect) produced by iron oxide (Bulte et al. 2004). The SPIO particles range between 50 and 100 nm in diameter and two characteristics in particular make superparamagnetic nanoparticle/MR imaging a technique with broad applications. First, methods have been developed for efficient SPIO cell labelling. Either nanaoparticles are being coated with a dendrimer that confers membrane permeability or a SPIO, such as Feredex, is transfected into cells by means of transfection reagents. Importantly, these passive labelling strategies are applicable to many different cell types, including resting stem cells. The utility of this approach is further underscored by recent efforts at clinical development; as Arbab et al. (2004) have described, a SPIO-based labelling preparation consisting of FDA approved materials. As an alternate labelling strategy, superparamagnetic nanoparticles can be modified with a TAT peptide, which facilitates transport across the cell membrane (Lewin et al. 2000). Second, in most cell types there is, thus far, little evidence of toxicity related to labelling. Recent work, however, suggested an adverse influence of the iron oxide label specifically on chondrocyte differentiation on mesenchymal progenitor cells, but an independent study could not confirm this finding (Kostura et al. 2004; Arbab et al. 2005). Since experimental conditions were different between those studies, no general conclusions can be derived as yet and further investigations are necessary. In addition to SPIO particles, micrometer-size particles harboring iron oxide (MPIOs) are available; they feature cell uptake through an inert divinyl benzene polymer shell of around 900-nm diameter and a larger amount of iron oxide per particle compared with SPIOs (Hinds et al. 2003).

The application of superparamagnetic nanoparticle/MR imaging is increasing and recent studies included imaging migration of locally injected iron oxide-labelled stem cells in the rat brain (Hoehn et al. 2002). Migration was also studied by Dodd et al. (2001), who imaged murine T-cells homing to the spleen. Although a clear reduction in signal intensity in the spleen was observed, the duration of the latter study did not exceed a 24-h period. A similar study reported that OVA-specific T-cells labelled with iron oxide nanoparticles migrated to and accumulated in an OVA-expressing melanoma xenograft over a period of 5 days (Kircher 2003). These labelling techniques clearly improved imaging the initial phase of T-cell migration following the adoptive transfer of the labelled lymphoid cells to sites providing a supportive microenvironment. However, ex-vivo labelling of T-cells with MR contrast is only transient and does not provide an opportunity to monitor their functional status, such as activation upon antigen recognition, cytokine secretion, proliferation and cytolytic functions. Nevertheless, MR imaging of iron oxide in general has recently been demonstrated to be of great clinical value (Harisinghani et al. 2003). As illustrated in Fig. 6, a clinical trial of MRI post systemic injection of lymphotropic nanocrystalline iron oxide in 33 patients affected by prostate cancer showed superior detection of lymph-node metastases compared with conventional proton MRI (Harisinghani et al. 2003).

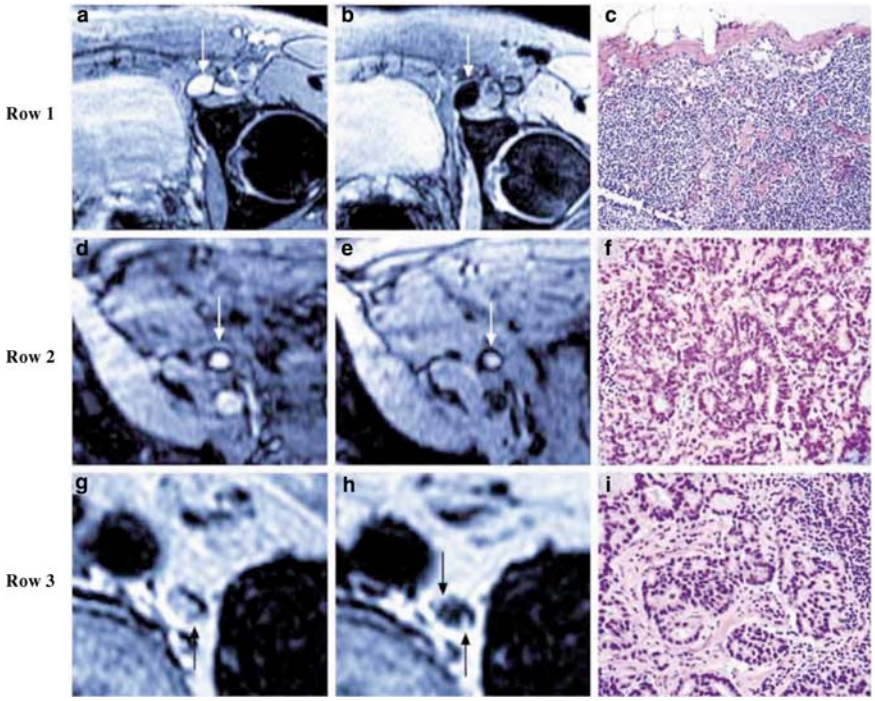

Fig. 6 a–i Non-invasive detection of clinically occult lymph-node metastases in prostate cancer by MRI using lymphotropic superparamagnetic nanoparticles. *Row 1:* Compared with conventional MRI **a**, MRI obtained 24 h after the administration of lymphotropic superparamagnetic nanoparticles **b** shows a homogeneous decrease in signal intensity due to the accumulation of lymphotropic superparamagnetic nanoparticles in a normal lymph node in the left iliac region (*arrow*). Panel **c** shows the corresponding histological findings of the normal lymph node (hematoxylin and eosin, ×125). *Row 2:* Conventional MRI shows high signal intensity in an unenlarged iliac lymph node completely replaced by tumour (*arrow* in **d**). Nodal signal intensity remains high indicated infiltration of tumour (*arrow* in **e**). Panel **f** shows the corresponding histologic findings and confirms the presence of tumour within the node (hematoxylin and eosin, ×200). *Row 3:* Conventional MRI shows high signal intensity in a retroperitoneal node with micrometastases (*arrow* in **g**). MRI with lymphotropic superparamagnetic nanoparticles demonstrates two hyperintense foci (*arrows* in **h**) within the node, corresponding to 2-mm metastases. Corresponding histological analysis confirms the presence of adenocarcinoma within the node (**i** hematoxylin and eosin, ×200). (Adapted from Harisinghani et al. 2003)

2.3 Indirect Molecular Imaging

Indirect imaging strategies are a little more complex. One example of indirect imaging that is now being widely used is reporter gene imaging. It requires "pre-targeting" (delivery) of the reporter gene to the target tissue (by transfection/transduction), and it usually includes transcriptional control components that can function as "molecular genetic sensors" that initiate reporter gene expression. This strategy

has been widely applied in optical- (Contag et al. 1998; Rehemtulla et al. 2000; Hoffman 2005) and radionuclide-based imaging (Tjuvajev et al. 1995b, 1996, 1998; Gambhir et al. 1998, 1999), and to a lesser degree for MR (Weissleder et al. 1997; Louie et al. 2000) imaging. Early reporter gene imaging approaches required post-mortem tissue sampling and processing (Overbeek et al. 1985; Forss-Petter et al. 1990), but more recent studies have emphasised non-invasive imaging techniques involving live animals and human subjects (Halbhuber and Konig 2003).

A general paradigm for non-invasive reporter gene imaging using radiolabelled probes was initially described in 1995 (Tjuvajev et al. 1995b) and is shown diagrammatically in Fig. 7. A simplified cartoon of a reporter gene is shown in Fig. 7a, and a representation of different reporter genes for imaging transduced cells is shown in Fig. 7b. This paradigm requires the appropriate combination of a reporter transgene and a reporter probe. The reporter transgene can encode a receptor [e.g. hD2R (human dopamine D2 receptor; Liang et al. 2001) and hSSTR2 (human somatostatin receptors; Rogers et al. 2000)], or a transporter [e.g. hNIS (human sodium iodide symporter; Haberkorn 2001) and hNET (human norepinephrine transporter; Altmann et al. 2003)], or a fluorescent protein [e.g. eGFP (enhanced green fluorescent protein; Chishima et al. 1997)] in addition to an enzyme, such as HSV1-tk (herpes simplex virus type 1 thymidine kinase; Tjuvajev et al. 1995b) [Fig. 7a (a), (b)] or luciferase (Contag et al. 1997) [Fig. 7a (a), (c)]. The reporter transgene usually codes for an enzyme, receptor or transporter that selectively interacts with a specific

Fig. 7 **a** Structure of a reporter gene construct and the indirect reporter imaging paradigm. The basic structure of a reporter gene complex is shown, expressing either HSV1-tk or luciferase. The control and regulation of gene expression is performed through promoter and enhancer regions that are located at the 5′ end ("up-stream") of the reporter gene. These promoter/enhancer elements can be "constitutive" and result in continuous gene expression ("always on"), or they can be "inducible" and sensitive to activation by endogenous transcription factors and promoters. Following the initiation of transcription and translation, the gene product — a protein — accumulates. **b** In this case the reporter gene product is the enzyme HSV1-tk, which phosphorylates selected thymidine analogues (e.g. FIAU or FHBG), whereas these probes are not phosphorylated by endogenous mammalian TK1. The phosphorylated probe does not cross the cell membrane readily; it is effectively "trapped" and accumulates is within transduced cells. Thus, the magnitude of probe accumulation in the cell (level of radioactivity) reflects the level of HSV1-tk enzyme activity and level of *HSV1-tk* reporter gene expression. **c** In this case, luciferase is the reporter gene product and expression is detected via its catalytic action resulting in production of bioluminescence. **b** Different reporter systems. The reporter gene complex is transfected into target cells by a vector (e.g. a virus). Inside the transfected cell, the reporter gene may or may not be integrated into the host-cell genome; transcription of the reporter gene to mRNA is initiated by "constitutive" or "inducible" promoters, and translation of the mRNA to a protein occurs on the ribosomes. The reporter gene product can be a cytoplasmic or nuclear enzyme, a transporter in the cell membrane, a receptor at the cell surface or part of cytoplasmic or nuclear complex, an artificial cell surface antigen, or a fluorescent protein. Often, a complimentary reporter probe (e.g. a radiolabelled, magnetic or bioluminescent molecule) is given and the probe concentrates (or emits light) at the site of reporter gene expression. The level of probe concentration (or intensity of light) is usually proportional to the level reporter gene product and can reflect several processes, including the level of transcription, the modulation and regulation of translation, protein-protein interactions, and post-translational regulation of protein conformation and degradation

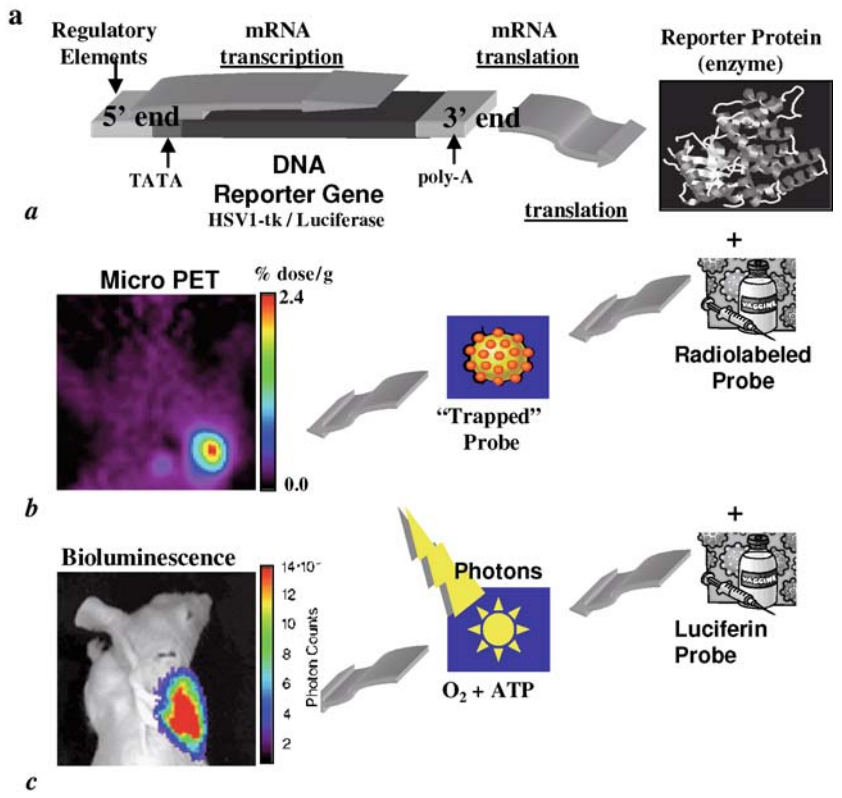
a
Regulatory Elements
mRNA transcription
mRNA translation
Reporter Protein (enzyme)
5' end
3' end
TATA
poly-A
DNA
Reporter Gene
HSV1-tk / Luciferase
translation
a
+
Micro PET
% dose/g
2.4
0.0
"Trapped" Probe
Radiolabeled Probe
b
+
Bioluminescence
Photons
Photon Counts
14·10⁻
12
10
8
6
4
2
O2 + ATP
Luciferin Probe
c

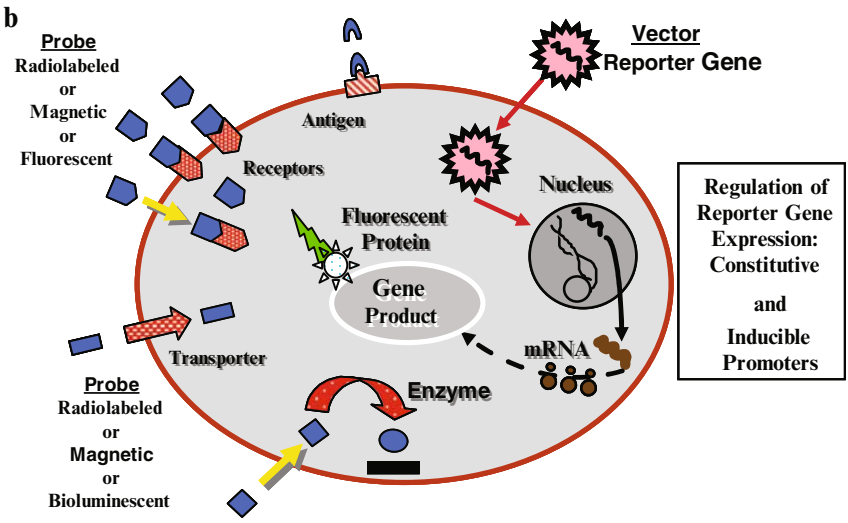
b
Probe
Radiolabeled or Magnetic or Fluorescent
Antigen
Receptors
Vector
Reporter Gene
Nucleus
Fluorescent Protein
Gene Product
mRNA
Transporter
Enzyme
Probe
Radiolabeled or Magnetic or Bioluminescent
Regulation of Reporter Gene Expression: Constitutive and Inducible Promoters

radiolabelled probe and results in its accumulation only in transduced cells. Alternatively, the enzyme (e.g. luciferase) will catalyse a reaction to yield light (photons) in the presence of substrate (e.g. luciferin, ATP and oxygen for firefly luciferase). Alternatively, the reporter gene product can be a fluorescent protein that can be imaged in vivo as well as ex vivo.

It may be helpful to consider the HSV1-tk reporter imaging paradigm as an example of an in-vivo radiotracer assay that reflects reporter gene expression [Fig. 7a (*a*), (*b*)]. Enzymatic amplification of the signal (e.g. level of radioactivity accumulation) facilitates imaging the location and magnitude of reporter gene expression. Viewed from this perspective, HSV1-tk reporter gene imaging with radiolabelled FIAU or FHBG is similar to imaging hexokinase activity with FDG. It is important to note that imaging transgene expression is largely independent of the vector used to shuttle the reporter gene into the cells of the target tissue; namely, any of several currently available vectors can be used (e.g. retrovirus, adenovirus, adeno-associated virus, lentivirus, liposomes, etc.).

A common feature of all reporter constructs (and their vectors) is the cDNA expression cassette containing the reporter transgene(s) of interest (e.g. *HSV1-tk*), which can be placed under the control of specific promoter-enhancer elements. The upstream promoter-enhancer elements can be used to regulate transcription of the reporter cDNA. The versatility of reporter constructs (and their vectors) is due in part to their modular design, since arrangements in the expression cassette can be varied to some extent. For example, reporter genes can be "always turned on" by constitutive promoters (such as *LTR*, *RSV*, *CMV*, *PGK*, *EF1*, etc.) and used to monitor cell trafficking by identifying the location, migration, targeting and proliferation of stably transduced cells. Reporter gene labelling provides the opportunity for repetitive imaging and sequential monitoring of tumour growth rate and response to treatment (Rehemtulla et al. 2000), as well as imaging metastases (Chishima et al. 1997). Alternatively, the promoter/enhancer elements can be constructed to be "inducible" and "sensitive" to activation and regulation by specific endogenous transcription factors and promoters (factors that bind to and activate specific enhancer elements in the promoter region of the reporter vector construct leading to the initiation of reporter gene transcription).

Considerable progress in reporter gene imaging has been achieved during the past 5 years. Important proof-of-principle experiments in small animals include the imaging of endogenous regulation of transcription (Doubrovin et al. 2001; Iyer et al. 2001b; Ponomarev et al. 2001), post-transcriptional modulation of translation (Mayer-Kuckuk et al. 2002), protein-protein interactions (Luker et al. 2002, 2003b; Ray et al. 2002), protein degradation and activity of the proteosomal ubiquination pathway (Luker et al. 2003a), apoptosis (Laxman et al. 2002), etc. Non-invasive imaging of viral (Gambhir et al. 1999; Tjuvajev et al. 1999), bacterial (Tjuvajev et al. 2001) and cell trafficking (Koehne et al. 2003), plus tissue-specific reporter gene imaging in prostate cancer (Zhang et al. 2002), hepatocytes (Green et al. 2002) and colorectal cancer cells have also been reported (Qiao et al. 2002).

2.3.1 Radiotracer Reporter Gene Imaging

HSV1-tk is the most widely used reporter gene for radiotracer-based molecular imaging, and has been used as a therapeutic "suicide" gene in clinical anti-cancer gene therapy trials as well as a research tool in gene targeting strategies. The HSV1-tk enzyme, like mammalian thymidine kinases, phosphorylates thymidine to thymidine-monophosphate (TdR). Unlike mammalian TK1, viral HSV1-tk can also phosphorylate modified thymidine analogues, including 2′-deoxy-2′-fluoro-5-iodo-1-[β]-D-arabinofuranosyluracil (FIAU), 2′-fluoro-5-ethyl-1-[β]-D-arabinofuranosyl-uracil (FEAU) as well as acycloguanosine analogs [e.g. acyclovir (ACV); ganciclovir (GCV); penciclovir (PCV)] that are not (or minimally) phosphorylated by eukaryotic thymidine kinases (Tjuvajev et al. 1995b). The resulting monophosphorylated compound is subsequently diphosphorylated and triphosphorylated by cellular kinases. The triphosphorylated compound can act as an inhibitor of DNA-polymerization, resulting in chain termination during DNA replication, leading to cell death. For this reason, *HSV1-tk* has been studied extensively as a therapeutic gene and used in gene therapy clinical trials that have been performed in the United States and Europe.

Several important issues were raised during these trials, including whether the viral transduction of the target tissue has been successful; what level of transgene expression is achieved in the target tissue; and what is the optimal time for beginning ganciclovir treatment. Another important clinical issue is monitoring for potential toxicity. Imaging the distribution and expression level of the therapeutic gene in non-target normal tissues provides a level of safety in individual patients undergoing gene therapy.

In the mid 1990s, a number of potential reporter probes for imaging *HSV1-tk* gene expression were studied in our laboratory (Tjuvajev et al. 1995b, 1996, 1998). After in-vitro determinations of HSV1-tk sensitivity and selectivity for FIAU, this compound was found to have good imaging potential and can be radiolabelled with a variety of radionuclides (^{11}C, ^{124}I, ^{18}F^{131}I, ^{123}I). FIAU contains a 2′-fluoro substitution in the sugar that impedes cleavage of the N-glycosidic bond by nucleoside phosphorylases. This results in a significant prolongation of the nucleoside in plasma and an increase in delivery of non-degraded radiolabelled tracer to the target tissues. The first series of imaging experiments involving *HSV1-tk*-transduced tissue and FIAU were performed in rats bearing intracerebral (i.c.) RG2 tumours using quantitative autoradiography (QAR) techniques (Tjuvajev et al. 1995a) (Fig. 8a). This was subsequently followed by gamma camera, single photon emission computed tomography (SPECT) (Fig. 8b) and positron emission tomography (PET) imaging studies (Fig. 8c). Other pyrimidine nucleoside probes for imaging viral thymidine kinase acitivity have been proposed (Fig. 9a).

Investigators from UCLA have used other radiolabelled compounds for PET imaging of HSV1-tk expression with the goal of developing methods for repetitive imaging (every 6–8 h) of the reporter protein. Their choice of acycloguanosine derivatives as reporter probes was based on the ability of these nucleosides to be radiolabelled with short-lived fluorine-18 ($t_{1/2} = 110\,\text{min}$) and no affinity to

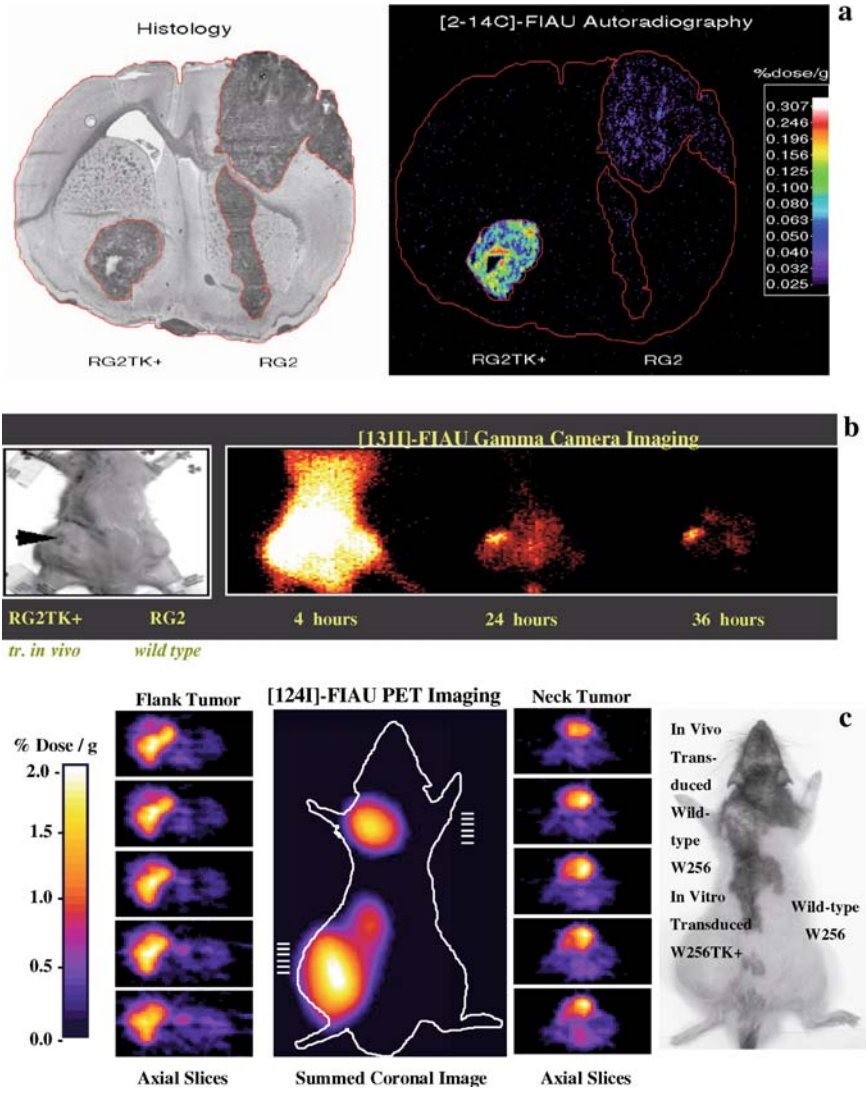

the mammalian TK-1. A list of ^{18}F-labelled acycloguanosine analogues is shown in Fig. 9b. After several years of comparative studies (Fyfe et al. 1978; Gambhir et al. 1998; Iyer et al. 2001a), a new radiolabelled acycloguanine, 9-(4-[^{18}F]fluoro-3-hydroxymethylbutyl)guanine or [^{18}F]FHBG (FHBG) (Alauddin and Conti 1998; Yaghoubi et al. 2001) was developed at USC. In parallel, the UCLA investigators evaluated a mutant HSV1-tk enzyme (HSV1-sr39tk) with increased acyclovir and ganciclovir suicidal efficacy. They showed higher affinity and uptake of [^{18}F]FHBG in HSV1-sr39tk transduced cells (Gambhir et al. 2000a). The mutant, HSV1-sr39TK, enhances [^{18}F]FHBG uptake by twofold compared with wild-type

Fig. 8 a Autoradiographic imaging HSV1-tk expression. A rat brain with a stably transduced RG2TK+ brain tumour in the left hemisphere and a wild-type (non-transduced) RG2 tumour in the right hemisphere is shown. The histology and autoradiographic images were generated from the same tissue section. Both tumours are clearly seen in the toluidine blue-stained histological section. Twenty four hours after i.v. administration of [^{14}C]FIAU, the RG2TK^{+} tumour is clearly visualised in the autoradiographic image, whereas the RG2 tumour is barely detectable; the surrounding brain is at background levels. (Adapted from Tjuvajev et al. 1995b). **b** Gamma-camera imaging HSV1-tk expression. Gamma-camera imaging was performed at 4, 24 and 36 h after [^{131}I]FIAU injection in an animals bearing bilateral RG2 flank xenografts; all images have been normalised to a reference standard (not shown in the field of view). The site of inoculation of HSV1-*tk* retroviral vector producer cells (gp-STK-A2) into the left flank xenograft is indicated by the *arrow*. The sequential images demonstrate wash-out of radioactivity from the body, with specific retention of activity in the area of gp-STK-A2 cell inoculation and transduction of RG2 tumour cells with the HSV1-tk reporter (see the 24- and 36-h images; readjustment of the pseudocolour-intensity scale demonstrated visualisation or the gp-STK-A2 flank tumour at 4 h, although background activity was high). The non-transduced contralateral xenograft (right flank) and other tissues did not show any retention of radioactivity. This sequence of images demonstrates the advantages of a "wash-out strategy" and late imaging with [^{131}I] – or [^{124}I]-labelled FIAU. Figure adapted from Tjuvajev et al. 1996 (Tjuvajev et al. 1996). **c** PET imaging of HSV1-tk expression. Three tumours were produced in rnu rats. A W256TK^{+} (positive control) tumour was produced from stably transduced W256TK^{+} cells and is located in the left flank, and two wild-type W256 tumours were produced in the dorsum of the neck (test) and in the right flank (negative control). The neck tumour was inoculated with 10^{6} gp-STK-A2 vector-producer cells (retroviral titre: 10^{6}–10^{7} cfu/ml) to induce HSV1-*tk* transduction of the tumour wild-type in vivo. Fourteen days after gp-STK-A2 cell inoculation, no carrier added [^{124}I]FIAU (25 µCi) was injected i.v. and PET imaging was performed 30 h later. Localisation of radioactivity is clearly seen in left flank tumour (positive control) and in the in-vivo transduced neck tumour (test), but only low background levels of radioactivity were observed in the right flank tumour wild-type (negative control). (Adapted from Tjuvajev et al. 1998)

HSV1-tk, thus improving the imaging capabilities of the enzyme. However, differences exist between the sensitivity and specificity of [^{124}I]FIAU and [^{18}F]FHBG with respect to wild-type HSV1-tk (Tjuvajev et al. 2002) and HSV1-sr39tk (Min et al. 2003).

One example of a reporter system involving a transporter is the sodium iodide symporter (NIS). Since cloning of the *NIS* gene in 1996 (Dai et al. 1996), *NIS* was considered an attractive imaging reporter gene (Dai et al. 1996; Boland et al. 2000). There are several distinct advantages for using *NIS* as a reporter gene. First, the distribution of endogenous NIS protein is limited in the body (thyroid and stomach are major exceptions); as a result, imaging of exogenous *NIS* gene expression can be performed in a variety of tissues due to low background activity. Second, NIS mediates the uptake of simple radiopharmaceuticals; therefore, complicated syntheses and labelling of substrate molecules are not required for imaging. Third, most of the radiotracers are specific only to NIS-expressing cells; therefore, background signal is significantly reduced. Fourth, NIS-mediated radiotracer uptake in target tissue is rapid, as is the clearance of radioactivity from both target and non-target tissues; this facilitates repetitive sequential imaging. Fifth, the human and murine genes of NIS have been cloned, which provides a non-immunogenic reporter system for human as well as rodent imaging studies.

a

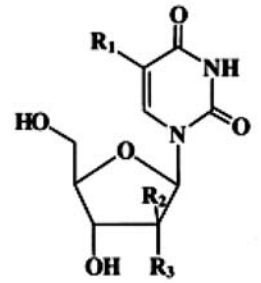

Probe	R1	R2	R3
FIAU	I	F	H
FIRU	I	H	F
FMAU	CH_3	F	H
IVFRU	CH_2=CH_2-I	H	F
IUdR	I	H	H
BrUdR	Br	H	H

b

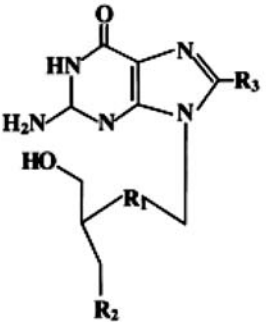

Probe	R1	R2	R3
GCV	O	OH	H
PCV	CH_2	OH	H
FGCV	O	OH	F
FPCV	CH2	OH	F
FHPG	O	F	H
FHBG	CH2	F	H

Fig. 9 a, b Substrates for HSV1-tk phosphorylation. **a** Pyrimidine nucleosides. **b** Acycloguanosine analogues. (Adapted from Tjuvajev et al. 2002)

An application of *hNIS* as a reporter gene was demonstrated by gamma-camera imaging myocardial gene transfer in living rats using adenoviral vectors and radioiodide (Shin et al. 2004). In this study, an adenovirus that expressed both NIS protein and enhanced green fluorescent protein (EGFP) (Ad.EGFP.NIS) was injected into the myocardium of living rats. Following ^{123}I scintigraphy demonstrated clear focal myocardial uptake at the Ad.EGFP.NIS injection site. Histological analysis confirmed the co-localisation of ^{123}I radioactivity, EGFP fluorescence and NIS staining. To develop a molecular imaging method suitable for monitoring viable cancer cells, another dual-imaging reporter gene system was constructed from two individual reporter genes — sodium iodide symporter (NIS) and luciferase (Lee et al. 2005). In parallel, our group has developed a self-inactivating retroviral vector containing a dual-reporter gene cassette (*hNIS-IRES2-GFP*) with the *hNIS* and *GFP* genes, separated by an internal ribosomal entry site (IRES) element; the expression cassette was driven by a constitutive CMV promoter. A stably transduced rat glioma (RG2) cell line was generated with this construct and used for in-vitro and in-vivo imaging studies of ^{131}I-iodide and $^{99\,m}TcO_4$-pertechnetate accumulation, as well as GFP fluorescence. The experiments demonstrated a high correlation between the expression of hNIS and GFP. Gamma-camera imaging studies performed on RG2 *hNIS-IRES2-GFP* tumour-bearing mice revealed that the *IRES*-linked dual reporter gene is functional and stable (Che et al. 2005).

The first successful reporter gene imaging study in patients was performed in Cologne using a *HSV1-tk* liposomal vector, [^{124}I]FIAU and PET to monitor *HSV1-tk* suicide gene therapy of high-grade brain tumours (Jacobs et al. 2001b). *HSV1-tk* gene expression was visualised in only one of six patients who received an intratumoural injection of the vector (Fig. 10.). Later on, [^{18}F]FHBG was studied in normal human volunteers and the biodistribution, bio-safety, and dosimetry was determined; it was found to be safe and potentially useful for human applications (Yaghoubi et al. 2005). More recently, the HSV1-sr39tk/[^{18}F]FHBG PET imaging system has been used to monitor thymidine kinase gene expression after intratumoural injection of the first-generation recombinant adenovirus in patients with hepatocellular carcinoma (Penuelas et al. 2005). Transgene expression in the tumour was dependent on the injected dose of the adenovirus and was detectable by PET during the first hours after administration of the radiotracer in all patients, who received $\geq 10^{12}$ viral particles (Fig. 10b). Non-specific expression of the transgene was not detected in any distant organs, or in the surrounding liver tissue in any of these studied cases. These results illustrate that PET imaging may help in the design of gene-therapy strategies and in the clinical assessment of new-generation vectors. Non-invasive monitoring of the distribution of transgene expression over

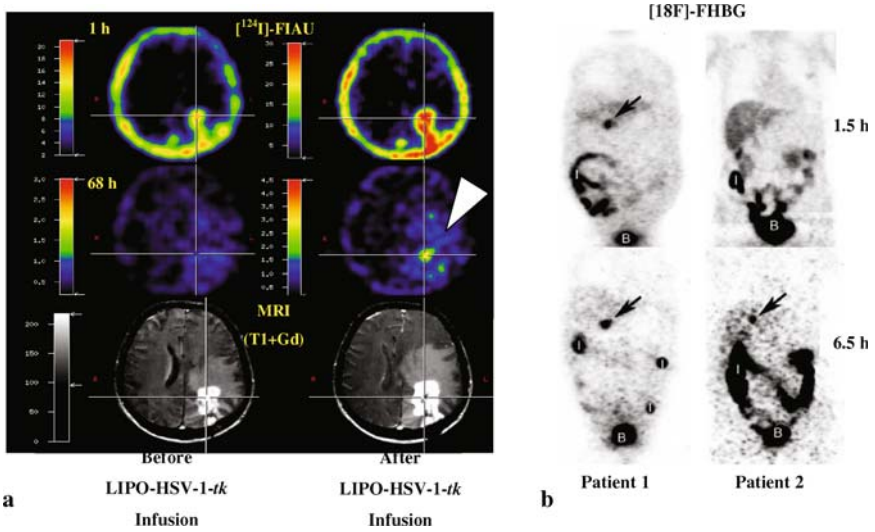

Fig. 10 **a** *HSV1-tk* reporter gene imaging in patients after liposome-*HSV1-tk*-complex transduction. Co-registration of [^{124}I]FIAU-PET and MRI before (*left column*) and after (*right column*) *HSV1-tk* vector application. A region of specific [^{124}I]FIAU retention (at 68 h) within the tumour is visualized (*white arrow*). This tumour region showed signs of necrosis (*cross hairs, right column*) after ganciclovir treatment. (Adapted from Jacobs et al. 2001b). **b** Adenoviral transgene (*HSV1-tksr39*) expression in patients with liver cancer. Coronal PET images 1.5 and 6.5 h after injection of [^{18}F]-FHBG (48 h after 2×10^{12} AdV-*tk*). Localisation of [^{18}F]-FHBG in the treated lesion was variable in the early images, but could be seen at 6.5 h in all patients (*arrow*). (Adapted from Penuelas et al. 2005)

time is highly desirable and will have a critical impact on the development of standardised gene therapy protocols and on efficient and safe vector applications in human beings. It is most likely that [^{124}I]FIAU and [^{18}F]FHBG will be the radiolabelled probes that will be introduced into the clinic for the imaging of *HSV1-tk* gene expression.

2.3.2 Optical-reporter gene imaging

Optical (bioluminescence and fluorescence) reporter systems have received increased attention recently, because of their efficiency for sequential imaging, operational simplicity, and substantial cost benefits.

Bioluminescence reporter genes

Bioluminescence reporter genes are being widely used for whole-body imaging in small animals. Luciferin and luciferase are generic terms, but not all luciferases exhibit sequence homology between the different classes. The most commonly used bioluminescence reporter systems include the firefly (FLuc) or *Renilla* (RLuc) luciferase genes (Yu et al. 2003). Useful luciferases have also been cloned from jellyfish (*Aequorea*), sea copepod (*Gaussia*; GLuc), corals (*Tenilla*), click beetle (*Pyrophorus plagiophthalamus*) and several bacterial species (*Vibrio fischeri, V. harveyi*). As with nuclear and magnetic resonance reporter systems, bioluminescence imaging depends on the delivery of a specific substrate to the reporter gene expressing cells. Further, the light emitting bioluminescence reaction catalysed by luciferases depends on the presence of oxygen (Wilson and Hastings 1998) and, for example, in the case of FLuc, additionally on the co-factor ATP. The firefly and *Renilla* luciferase reporter systems, in combination with their corresponding luminescent substrates (luciferin and coelenterazine), have several advantages for imaging small living animals. Autobioluminescence in most cases is essentially non-existent and results in very low background light emission; this contributes to the very high sensitivity and specificity of this optical imaging technique (Bhaumik and Gambhir 2002; Wu et al. 2002). Semi-quantitative accuracy and reproducibility requires that the luciferin, ATP and oxygen levels are *not* rate determining, but rather are in excess. Under these conditions, the photon emission flux (light intensity) is directly related to reporter gene expression and the level of reporter gene product; namely, luciferase. Another potential concern is the fact that the substrate for *Renilla* luciferase, coelenterazine, is a substrate for the MDR1 transporter. It has recently been shown that coelenterazine is rapidly exported from cell lines that express MDR1, and this could impact on the photon emission flux from the coelenterazine-*Renilla* luciferase reporter system in these cells (Pichler et al. 2004). In-vivo bioluminescence imaging has been successfully applied to monitor the growth of individual tumours (Fig. 11) and to assess the function of many novel reporter systems (see below). However, care must be exercised when comparing

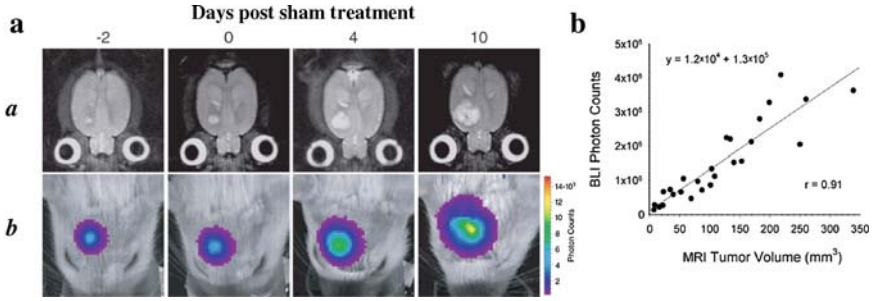

Fig. 11 a, b Kinetics of intracranial glioma growth. **a** $9L^{Luc}$ cells were implanted intracerebrally and tumour progression was monitored with MRI (*row a*) and BLI (*row b*). The days of post-sham treatment on which the images were obtained are indicated at the *top*. The MR images are T_2-weighted and are of a representative slice from the multislice dataset. **b** The *scale to the right* of the BL images describes the colour map for luminescent signal. Correlation of tumour volume with in vivo photon emission is shown where tumour volume was measured from T_2-weighted MR images and plotted against total measured photon counts. The relationship between the two measurements was defined by regression analysis ($r = 0.91$). (Adapted from Rehemtulla et al. 2000)

different tumours (or sites of bioluminescence) because of the significant loss of signal due to the scatter and absorption of emitted photons that can vary over several logs with distance from the surface and tissue type (e.g. lung vs liver vs bone).

Fluorescent protein-based reporter systems

Fluorescent protein-based reporter systems have also become very popular during the 1990s, especially for in-vitro and embryogenesis studies. For example, green fluorescent protein (GFP) has evolved from a little known protein to a common widely used tool in molecular biology and cell biology. It started with different spectral shifted variants of *Aequorea victoria* GFP (*GFP*), including an enhanced GFP (*eGFP*) (Levy et al. 1996; Lalwani et al. 1997; Ellenberg et al. 1999; Matz et al. 1999; Falk and Lauf 2001; Hadjantonakis and Nagy 2001; Labas et al. 2002). These GFP variants are particularly useful because of their stability and the fact that the chromophore is formed by autocatalytic cyclization. Furthermore, it appears that fusion of GFP to other proteins does not significantly alter its fluorescence properties or the intracellular location of the fusion protein (Ponomarev et al. 2003, 2004). A number of red fluorescent proteins including *Discosoma species* (*dsRed1* and *dsRed2*) (Campbell et al. 2002; Mathieu and El-Battari 2003) and *Heteractis crispa* (*HcRed*) (Gurskaya et al. 2001) have also been described. Employing DsRed as a genetically encoded fusion tag has been limited because of two critical problems: obligate tetramerization and incomplete maturation. Several attempts have been made to overcome these shortcomings, including genetic modification and creation of DsRed2 and DsRed-Express (T1) proteins. Significant progress has been achieved in resolving the problem of tetramerization by transforming DsRed

into a far-red dimer, HcRed1, which was generated on the basis of the chromoprotein from *Heteractis crispa* (Gurskaya et al. 2001). Roger Y. Tsien's group have presented the step-wise evolution of DsRed to a dimer and then either to a genetic fusion of two copies of the protein, i.e. a tandem dimer, or to a true monomer, designated mRFP1 (monomeric red fluorescent protein) (Campbell et al. 2002). Recently, the same group has reported on the development of a novel mutant mRFP monomeric fluorescent protein called mPlum with an emission wavelength 649 nm, which is 37 nm longer than the peak of the original mRFP and 12 nm beyond the previous tandem dimer t-HcRed1 (Wang et al. 2004).

Fluorescence imaging has been shown to be useful for various in-vitro applications, such as: (1) monitoring the gene expression, (2) tracking of the protein of interest: its expression, localisation, movement, interaction and functional activity within the cell, (3) identifying and selecting cells by FACS analysis and sorting (e.g. expression of p53 in tissue sections at the microscopic level by in-situ fluorescence imaging (Doubrovin et al. 2001), (4) tracking the movement of labelled cells, proteins and different organelles using photoswitchable proteins (Chudakov et al. 2004) and (5) for cost-effective in-vitro assays that can be used to validate the function and sensitivity of inducible reporter systems containing multi-modality reporter genes (see below).

The brightness of all fluorescent proteins is determined by several variable factors, including the speed and efficiency of protein folding and maturation, the extinction coefficient, quantum yield and photostability of the protein, as well as the optical properties of the imaging set-up and camera. Genetically modified fluorescent proteins can be optimised for mammalian cells with good expression at 37° C (Fig. 12) (Shaner et al. 2004), whereas other proteins may fold less efficiently or be rapidly degraded. Experiments in bacteria and mammalian cells have shown that chaperones can have a substantial effect on the folding and maturation efficiency of fluorescent proteins. An additional factor affecting the maturation of fluorescent proteins in living organisms is the presence or absence of molecular oxygen. Fluorescence is usually prevented or reduced under anoxic conditions, although fluorescence persists under hypoxia conditions (Shaner et al. 2005). Many wild-type fluorescent proteins have tetrameric structures which can cause the protein aggregation and toxicity. More recently engineered monomers or tandem dimers of tetrameric fluorescent proteins have been shown to be less toxic and more suitable for mammalian cell studies. There are some genetically modified proteins that very bright [e.g. mPlum, mCherry, and Emerald proteins (Shaner et al. 2005)]. Although the present set of fluorescent proteins gives researchers a variety of options in their studies, there is still room for improvement. In the future, monomeric proteins with greater brightness and photostability will allow for more intensive imaging experiments in thick tissue and whole animals.

Limitations of fluorescence reporter imaging include the requirement for an external source of light and the exponentially decreasing intensity of light with increasing depth of the target. Endogenous autofluorescence of tissues frequently results in substantial background emissions that limit the sensitivity and specificity of fluorescence imaging techniques, and this contributes to an important advantage

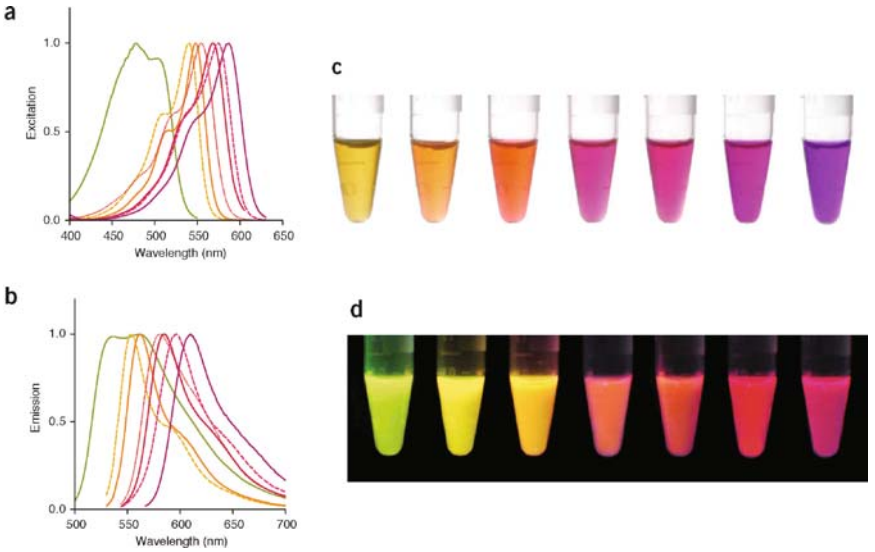

Fig. 12 a–d Excitation and emission spectra for new red fluorescent protein (RFP) variants. Spectra are normalised to the excitation and emission peak for each protein. Excitation **a** and emission **b** curves are shown as *solid or dashed lines* for monomeric variants and as a *dotted line* for dTomato and tdTomato, with colours corresponding to the colour of each variant. Purified proteins (*from left to right:* mHoneydew, mBanana, mOrange, tdTomato, mTangerine, mStrawberry, and mCherry) are shown in visible light **c** and fluorescence **d**. The fluorescence image is a composite of several images with excitation ranging from 480 to 560 nm. (Adapted from Shaner et al. 2004)

of bioluminescence over fluorescence reporters. However, the use of selective filters or the application of spectral analysis can significantly reduce the contribution of autofluorescence to the acquired images. Nevertheless, in-vivo bioluminescence reporter imaging remains more sensitive than in-vivo fluorescence reporter imaging.

Luciferase may be well suited to monitor transcription; due to its relatively fast induction (Kolb et al. 2000) and to the considerable short biological half-life of luciferin and luciferase (Thompson et al. 1991). This is an advantage compared with the longer-lived eGFP. However, short-lived (rapidly degradable) variants of eGFP have been recently developed, and eGFP can be used for higher resolution imaging in cells in vitro. Combining these reporter genes into a single gene could provide additional tools for the analysis of cancer cells in vivo and ex vivo. Such a dual-function reporter gene was created and the single encoded protein was shown to be fluorescent and bioluminescent.

Multi-modality nuclear and optical reporter imaging

The coupling of a nuclear reporter gene (e.g. *HSV1-tk*) with an optical reporter gene (e.g. *eGFP*) has been reported (Jacobs et al. 2001a). More recently, a series of HSV1-tk/eGFP mutants were developed with altered nuclear localisation

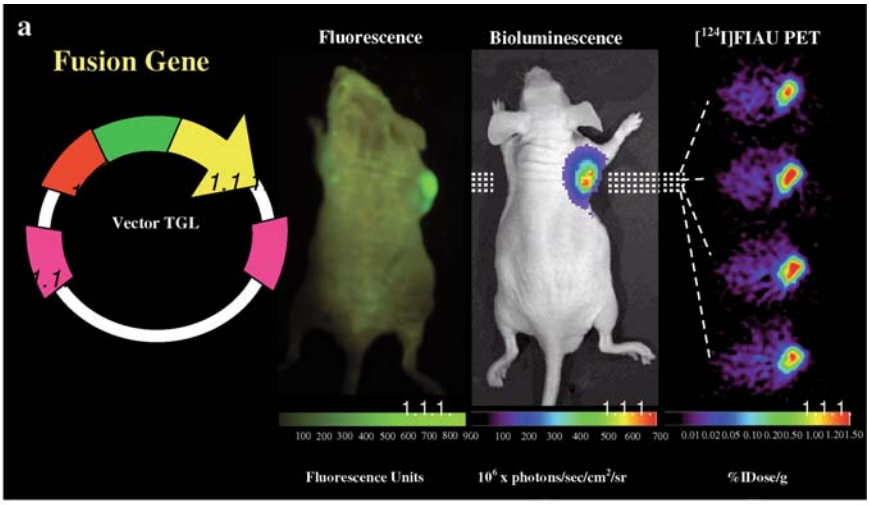

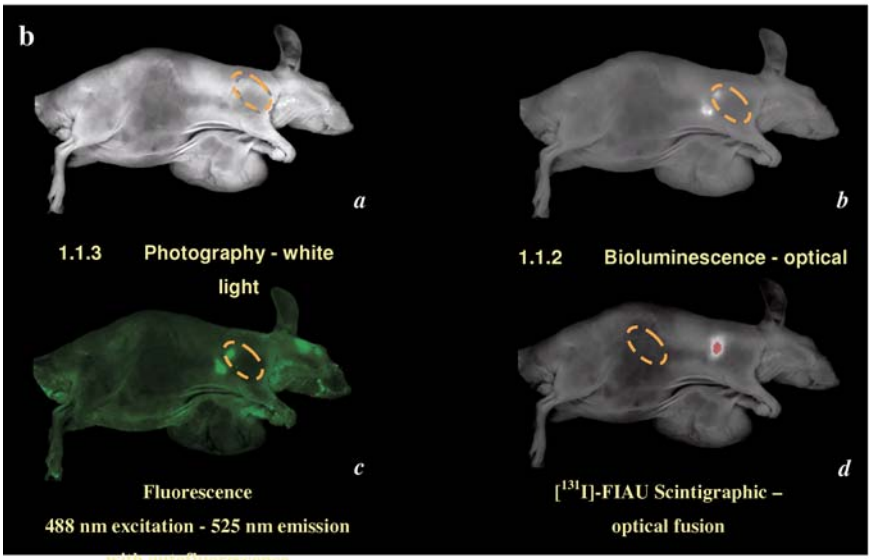

and better cellular enzymatic activity to optimise the sensitivity for imaging *HSV1-tk/eGFP* reporter gene expression (Ponomarev et al. 2003). The *HSV1-tk/eGFP* reporter gene has been introduced into several different reporter systems to assess different molecular pathways (Doubrovin et al. 2001; Ponomarev et al. 2001). Furthermore, a mutant thymidine kinase (HSV1-sr39tk)/*Renilla* luciferase (RL) fusion reporter construct $(tk_{20}rl)$ was recently developed for both nuclear and optical imaging (Ray et al. 2003). This study demonstrated the specificity and sensitivity of

Fig. 13 a, b Non-invasive multimodality imaging. **a** Non-invasive, multimodality imaging of mice bearing subcutaneous xenografts produced from nesHSV1-tk/eGFP-cmvFluc transduced U87 cells (right shoulder) and wild-type (non-transduced) U87 cells (left shoulder). Whole-body fluorescence imaging (*a*), whole-body bioluminescence imaging (*b*), and axial microPET images of [^{124}I]FIAU accumulation obtained at the levels indicated by the *dotted white lines* (*c*) are shown for the same mouse. (Adapted from Ponomarev et al. 2004). **b** Sequential images of a different mouse were obtained on a Kodak R2000MM multimodal imaging system. A white light photograph was initially obtained showing a small nesHSV1-tk/eGFP-cmvFluc transduced U87 xenograft (*dashed outline*) in the right shoulder and a large non-transduced U87MG xenograft located in the right shoulder and extending beneath the animal (*a*). This was followed by whole-body fluorescence imaging without correction for autofluorescence (*b*), whole-body bioluminescence imaging (*c*), whole-body scintigraphic imaging of [^{131}I] radioactivity, 24 h after i.v. [^{131}I]FIAU administration (*d*). All images were obtained from the same mouse at the same imaging session, and the mouse remained stationary between each imaging session. Note that (*c*) and (*d*) include optical fusion with the white-light photograph shown in (*a*)

bioluminescence imaging and showed a good correlation between the nuclear (microPET) and optical (CCD camera) read-outs of the dual reporter system.

More recently, triple-reporter constructs (e.g., HSV1-TK/eGFP/Luc or TGL), have been developed (Ray et al. 2003; Ponomarev et al. 2004). The map of the plasmid is shown in Fig. 13. A single reporter construct (vector) with a gene product(s) that can be assayed by three different imaging technologies (nuclear, fluorescence and bioluminescence) combines the benefits of each modality. Such systems facilitate the development, validation and testing of new reporter systems in small animals, as well as provide preliminary data that will facilitate the translation of such studies into humans. Using dual or triple modality reporter constructs (PET, fluorescence and bioluminescence) overcomes many of the shortcomings of each modality alone. Although optical imaging does not yet provide optimal quantitative or tomographic information, these issues are not limiting for PET-based reporter systems and PET animal studies are more easily generalised to human applications. Multi-modality reporters have been shown to facilitate the development, validation and testing of new reporter systems in small animals (Gambhir 2002; Blasberg and Tjuvajev 2003), as well as provide preliminary data that will facilitate the translation of such studies into humans.

3 Applications of Reporter Gene Imaging

Reporter gene imaging can provide non-invasive assessments of endogenous biological processes in living subjects. For example, imaging the *transcriptional regulation* of endogenous genes in living animals using non-invasive imaging techniques can provide a better understanding of normal and cancer-related biological processes. Recent papers from our group have shown that p53- and HIF-1 (hypoxia inducible factor-1)-dependent gene expression can be imaged in vivo with PET and by in-situ fluorescence (Doubrovin et al. 2001; Serganova et al. 2004). Retroviral

vectors were generated by placing the *HSV1-tk/eGFP*, a dual-reporter gene, under control of a several repeats of the p53 protein (transcription factor) (Doubrovin et al. 2001), and several repeats of the hypoxia response element (HRE, a specific response element for HIF-1) (Serganova et al. 2004) (see below).

Imaging endogenous gene expression may be hampered when *weak promoters*, in their usual *cis* configuration, a re-used to activate the transcription of the reporter gene. This results in insufficient transcription of the reporter gene. To address this limitation, a "two-step transcriptional amplification" (TSTA) approach can be used to enhance transcriptional activity. TSTA was used to image activation of the androgen-responsive prostate-specific antigen promoter (PSE) with firefly luciferase and mutant herpes simplex virus type 1 thymidine kinase (HSV1-sr39tk) reporter genes in a prostate cancer cell line (LNCaP) (Zhang et al. 2002). Further improvements of the androgen-responsive TSTA system for reporter gene expression were made using a "chimeric" TSTA system that uses duplicated variants of the prostate-specific antigen (PSA) gene enhancer to express GAL4 derivatives fused to one, two, or four VP16 activation domains. A very encouraging result was the demonstration that the TSTA system was androgen concentration sensitive, suggesting a continuous rather than binary reporter response. Another study (Qiao et al. 2002) validated methods to enhance the transcriptional activity of the carcinoembryonic antigen (CEA) promoter using the TSTA principle. To increase promoter strength while maintaining tissue specificity, a recombinant adenovirus was constructed which contained a TSTA system with a tumour-specific CEA promoter driving a transcription transactivator, which then activates a minimal promoter to drive expression of the HSV1-tk suicide/reporter gene. This ADV/CEA-binary-HSV1-tk system resulted in equal or greater cell killing of transduced cells by ganciclovir in a CEA-specific manner, compared with ganciclovir killing of all cells transduced with a CEA-independent vector containing a constitutive viral promoter driving HSV1-tk expression (ADV/RSV-tk). However, as observed with the PSE-TSTA reporter system above, the in-vivo imaging comparison of the TSTA and *cis* reporter systems showed substantially less dramatic differences than that obtained by the in-vitro analyses.

Gene expression levels are also regulated by post-transcriptional modulation, including the translation of mRNA. A recent study demonstrated that imaging post-transcriptional regulation of gene expression is feasible. This was shown by exposing cells to antifolates and inducing a rapid increase in the levels of the enzyme dihydrofolate reductase (DHFR). Several studies indicated that the DHFR binds to its own mRNA in the coding region, and that inhibition of DHFR by methotrexate (MTX) releases the DHFR enzyme from its mRNA. Consequently, this release results in an increase in translation of DHFR protein. In addition to the described translational regulation of DHFR in cancer cells exposed to MTX, increased levels of DHFR also result through *DHFR* gene amplification, a common mechanism of acquired resistance to this drug. In contrast to rapid translational modulation of DHFR, gene amplification occurs in response to chronic exposure to antifolates, and elevated cellular levels of DHFR result from transcription of multiple *DHFR* gene copies. Recently, Mayer-Kuckuk et al. (2002) utilised imaging to

show that the antifolate-mediated regulation of DHFR indeed occurs in vivo. For this study, a mutant DHFR was tagged with the reporter gene *HSV1-tk*; a modification that neither abolished the DHFR response to methotrexate or trimetrexate, nor compromises the activity of the robust *HSV1-tk* reporter gene. Regulation of the DHFR-HSV1-TK fusion protein could be visualised in PET imaging studies that were performed on nude rats bearing *DHFR-HSV1-tk*-transduced HCT-8 xenografts. In this model, systemic administration of antifolate results in increased accumulation of the DHFR-HSV1-TK fusion protein in tumour tissue. Positron emission tomography of this increase was achieved after injection of the HSV1-tk substrate [^{124}I]FIAU and tracer clearance. The results of this in-vivo imaging were consistent with complementing in-vitro experiments and indicated that the increase in the fusion reporter protein DHFR-HSV1-TK was occurring at a translational level, rather than at the transcriptional level.

3.1 Tissue Hypoxia: The Biological Basis for Indirect Imaging of Hypoxia

Given the importance of hypoxia in cancer progression and therapy, there has been a long-standing interest in developing non-invasive imaging methodologies to detect and assess tumour hypoxia. However, tumour hypoxia is a spatially and temporally heterogeneous phenomenon, resulting from the combined effect of many factors, including tumour type and volume, disease site (specific organ or tissue), regional microvessel density, blood flow, oxygen diffusion and consumption rates, etc. The most important regulatory factor of the hypoxia signalling pathway in cells is hypoxia-inducible transcription factor-1 (HIF-1). HIF-1 mediates adaptive responses to reduced O_2 availability. HIF-1 is a heterodimeric protein consisting of an oxygen-regulated α-subunit and a stable β-subunit (Wang and Semenza 1995). HIF-1α undergoes rapid turnover (half-life is less than 5 min) in the presence of oxygen, being degraded by the ubiquitin-proteasome pathway through the interaction with the VHL (von Hippel-Lindau) protein (Ivan et al. 2001). VHL recognition of the HIF-1α subunit is dependent on the hydroxylation of conserved proline residues within HIF-1α, that occurs only when oxygen is available (Salceda and Caro 1997; Kaelin 2005).

We developed an inducible reporter system that was sensitive to hypoxia and could be monitored by non-invasive imaging (Serganova et al. 2004). Up-regulation of the HIF-1 transcriptional factor was demonstrated and correlated with the expression of dependent downstream genes (e.g. *VEGF*) (Fig. 14). PET imaging of HIF-1 transcriptional activity in tumours using this reporter system was developed and validated (Serganova et al. 2004), and this reporter system could be used to assess the effects of radiation, new drugs or other novel therapeutic paradigms that impact on the HIF-1 signalling pathways.

In the absence of an imaging technique to directly determine the partial oxygen pressure (pO_2) in tissue, current non-invasive methodologies must be corroborated.

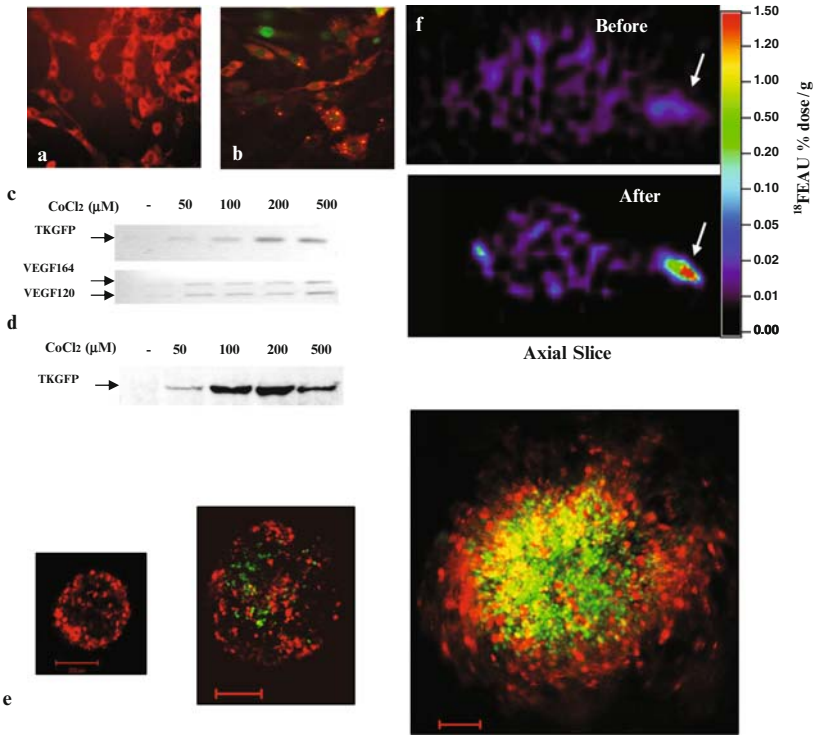

Fig. 14 a–f Characterisation of a hypoxia-sensitive specific reporter system. Fluorescence microscopy of #4C6 reporter cells (cells were transduced with a double reporter vector bearing a constitutively expressed reporter fusion *dsRed2/XPRT* and a hypoxia regulated *HSV1-tk/GFP* fusion gene) under base-line conditions **a** and following exposure to 200 μM $CoCl_2$ for 24 h **b**. VEGF and HSV1-tk/GFP expression in response to hypoxic conditions. **c** Agarose-gel electrophoresis of the RT-PCR products was performed to validate a hypoxia dependent reporter system (HSV1-tk/GFP). **d** Western blotting of the expression level of HSV1-tk/GFP confirms the integrity of the reporter system. Assays were performed 24 h after exposure to different concentrations of $CoCl_2$. **e** Sequential confocal microscopic images of the multi-cellular spheroid from reporter #4C6 cells during different phases of growth (*bar* 200 μm). Normoxic cells (small spheroid and periphery of larger spheroids) show only red-fluorescing cells and demonstrate no HIF1 transcriptional activity. Hypoxic TKGFP-fluorescing cells are clearly detectable within the central region when the spheroid grows to 350–400 μm in diameter. At a significantly larger size, this central region becomes necrotic as evidenced by the absence of cell fluorescence. In-vivo microPET imaging of ischemia-reperfusion injury-induced HIF-1 transcriptional activity. **f** Axial PET images of HIF-1-mediated HSV1-TK/GFP expression in s.c. #4C6 xenografts growing in both anterior limbs of the same mouse before and after tourniquet application to the left anterior limb proximal to tumour. The s.c. #4C6 tumour xenograft growing in the right limb was not affected and served as a control. (Adapted from Serganova et al. 2004)

Validation experiments are frequently performed by comparisons with direct pO_2 probe measurement (considered the "gold standard") or by immunohistochemical techniques, which provide detailed microdistribution data of relative (not absolute) pO_2 level. Physical measurement of pO_2 levels using polarographic oxygen

electrodes (Brizel et al. 1996; Hockel et al. 1996; Nordsmark et al. 1996) have been shown to be of prognostic value. These devices provide a direct measure of pO_2 at a specific, but this method is invasive and provides selected pO_2 data along a series of individual sampling tracks with an inherent limitation of tumour sampling. Immunohistochemical (IHC) methods are based on antibody detection of exogenous hypoxia markers, such as pimonidazole (Nordsmark et al. 2003) or EF5 (Koch and Evans 2003; Evans et al. 2004), that are injected into the patient prior to surgical resection of tissue (tumour). IHC methods yield microscopic information on hypoxia in relation to tumour histology. However, such data requires the acquisition of tissue specimens by invasive time-consuming IHC techniques and provides only relative pO_2 information. In addition, only a small number of sections can be realistically processed per patient; thus, immunohistochemical methods are inherently limited and subject to sampling errors. These limitations have spurred enthusiasm for the development of non-invasive imaging methods that provide tomographic visualisation of tissue hypoxia in tumours and can be repeated. Endogenous molecular markers of tumour oxygenation have been suggested and studied. In patients with cervical cancer patients HIF-1 might represent a reliable intrinsic marker for tumour hypoxia and prognosis (Bachtiary et al. 2003). GLUT-1 has also been shown to be an endogenous marker of hypoxia for oral squamous cell carcinoma and rectal carcinoma (Cooper et al. 2003; Oliver et al. 2004). Another a much cited endogenous marker of tumour oxygenation is carbonic anhydrase 9 (CA9) (Giatromanolaki et al. 2001). It was shown, that it can be a prognostic indicator in cervical cancer (Loncaster et al. 2001), and in invasive breast cancer studies (Colpaert et al. 2003). However, none of these markers can be universally used across many tumour types, because they are likely cell-type specific and are not reliable for the reasons discussed above.

The principal non-invasive approaches to imaging tumour hypoxia include magnetic resonance and radionuclide (PET and SPECT) imaging, but other techniques such as optical imaging or electron spin resonance are under investigation. For example, near-infrared (NIR) imaging detects tissue hypoxia as a decrease in the local blood pool oxyhemoglobin-deoxyhemoglobin ratio but with poor spatial resolution (Brun et al. 1997). Electron paramagnetic resonance imaging (EPRI) is a newly emerging MR imaging technology which can produce images of oxygen levels in normal and tumour tissues (Elas et al. 2003) and may soon develop into a more widely used method in studies of hypoxia. More conventional MR techniques include blood-oxygen-level-dependent (BOLD) imaging, which detects a change in tissue perfusion by the amount of oxygenated blood (Krishna et al. 2001), and has become widely used in fMRI applications (Hennig et al. 2003). However, BOLD cannot be used to determine the level of oxygen in tissues or characterise the molecular-genetic changes in tumour cells. NMR spectroscopy can detect increased lactate (a product of anaerobic glycolysis) and decreased ATP levels in ^{1}H and ^{31}P spectra, respectively, as well as tissue pH, but has poor sensitivity (in mmol range) and poor spatial resolution $(\sim 1\,cm^3)$ (Gillies et al. 2002).

Radionuclide-based imaging approaches, using a direct imaging strategy, claim a detection sensitivity which is several orders of magnitude higher than MR-based

techniques. However, the resolution of modern whole-body PET and SPECT systems ranges from 4 to 10 mm. PET can provide quantitative images of a variety of processes that are related to hypoxia (Lewis and Welch 2001). Using $^{15}O_2$ inhalation (Iida et al. 1996), parametric PET images of tissue oxygenation levels, regional oxygen extraction fraction and metabolic rate can be generated with much higher accuracy than with invasive measurements of oxygen tension in tissues (Gupta et al. 2002). PET imaging with $^{15}O_2$ is currently the "gold standard" for non-invasive imaging of tissue oxygen levels. However, it is not widely used for experimental or clinical imaging, due to the very short half-life of $^{15}O_2 (t_{1/2} \approx 2\,\text{min})$, which renders such studies (both animal and clinical) logistically and technically complex as well as expensive.

The more widely used clinical studies to image hypoxia using PET are based on 2-nitroimidazole halogenated tracers, such as ^{18}F-labeled misonidazole ([^{18}F]-FMISO) (Rasey et al. 1996). The nitroimidazoles become reduced in a hypoxic environment and then covalently bind to intra- and extracellular molecules, and the magnitude of their accumulation has been shown to be proportional to the level of hypoxia (Chapman et al. 1983). Several nitroimidozole compounds have been radiolabelled and studied as potential hypoxia imaging agents. Lehtio et al. (2004) evaluated the use of ^{18}F-fluoro-erythronitroimidazole (FETNIM) and tested it as a predictor of radiotherapy outcome. They reported that the data of [^{18}F]-FETNIM was suggestive but inconclusive. Another 2-nitroimidazole, 2-(2-nitro-1H-imidazol-1-yl)-N-(2,2,3,3,3-pentafluoropropyl) acetamide (EF5), has been successfully used as an immunohistochemical marker of hypoxia in surgical trials. PET images have been obtained with EF5 (Evans et al. 2000).

3.2 Imaging Adoptive Therapies

A non-invasive method for repetitive evaluation of adoptively administered cells benefits the assessment of current adoptive therapies in clinical use (e.g. bone marrow transplantation, immune cell and blood-derived progenitor cell-based therapies) as well as future adoptive therapies using stem cells. Individual patient monitoring would contribute to patient management by visualising the trafficking, homing-targeting and persistence of adoptively administered cells, as well as assess their functional activation, proliferation and cytokine expression. Such studies would significantly aid in the clinical implementation and management of new therapeutic approaches based on the adoptive transfer of immune cells, progenitor cells and stem cells.

In this section we will focus on adoptive T-cell monitoring, although the methods for non-invasive monitoring can be readily transferred other systems (e.g. bone marrow stromal cells or endothelial precursor cell). Non-invasive imaging of lymphocyte trafficking dates back to the early 1970s, when the first experiments were performed with extracorporeal labelling of lymphocytes using various metallic radioisotopes and chelation attachments to the cell surface (e.g. ^{111}In, ^{67}Co, ^{64}Cu, ^{51}Cr, $^{99\,m}$Tc) (Papierniak 1976; Gobuty 1977; Rannie 1977; Korf 1998; Adonai

2002). A major limitation of ex-vivo labelling of lymphocytes with radionuclides is the relatively low level of radioactivity per cell that can be attained by labelling cells. The exposure of cells to higher doses of radioactivity during labelling is also limited by radiotoxicity. Another shortcoming of ex-vivo radiolabelling is the short period for cell monitoring, which is limited by radioactivity decay and biological clearance.

The genetic labelling of cells for adoptive therapy monitoring provides substantial advantages for long-term monitoring and for assessing the functional status of the adoptively transferred cells. Retroviral-mediated transduction has proven to be one of the most effective means to deliver transgenes into T-cells and results in high levels of sustained transgene expression (Gallardo et al. 1997; Hagani 1999). Genetic labelling of lymphocytes with the luciferase (*FLuc*) reporter gene and non-invasive bioluminescence imaging (BLI) of mice has been reported (Hardy 2001; Zhang 2001). Costa et al. (2001) showed the migration of myelin basic protein specific, Luc-transduced $CD4^+$ T-cells in the central nervous system. The distribution of cytotoxic T-lymphocytes (CTL) can also be followed throughout the organism and monitored over time using BLI of Luc-expressing CTLs. The variable optical characteristics of tissue at different depths from the surface on the emitted photons must be recognised in any BLI assessment of cell trafficking. Nevertheless, BLI based on Luc expression has great potential in preclinical mouse-model studies, where high sensitivity, low cost, and technical simplicity are important for rapid screening.

The long-term trafficking and localisation of T-lymphocytes is an important component of the immune response, and in the elimination of abnormal cells and infectious agents from the body. Passive (ex vivo) labelling of T-cells with radioisotopes or magnetic labels can be unstable, is limited in long-term assessments and does not account for proliferation of activated T-cells in the body. Our group demonstrated the feasibility of long-term in-vivo monitoring of adoptively transferred antigen-specific T cells that were transduced to express a radiotracer-based reporter gene for non-invasive in-vivo PET imaging (Koehne 2003). EBV-specific T cells (CTLs) were obtained and stably transduced with a constitutively expressed dual reporter gene (*HSV1-tk/GFP* fusion gene). SCID mice bearing four tumours [(1) autologous HLA-$A0201^+$ EBV-transformed B cells (EBV BLCL); (2) allogeneic EBV BLCL expressing HLA-A0201 allele; (3) allogeneic HLA mismatched EBV BLCL; (4) EBV-negative HLA-$A0201^+$ B-cell acute lymphoblastic leukemia (B-ALL)] were treated with *HSV1-tk/GFP*-transduced EBV-specific CTLs. Specific accumulation and localisation of radioactivity was observed only in the autologous and allogeneic HLA-$A0201^+$ EBV-BLCL; no T-cell infiltration was seen in the allogeneic HLA-A0201-matched, EBV-negative B-ALL or HLA-mismatched EBV BLCL xenografts (Fig. 15). Sequential imaging over 15 days after T-cell injection permitted long-term monitoring of the *HSV1-tk/GFP*-transduced cells and demonstrated tumour-specific migration and targeting of the CTLs. Infusion of EBV-specific cytotoxic T-cells (CTLs) led to the elimination of subcutaneous autologous EBV-BLCL tumour and HLA-$A0201^+$ allogenic EBV-BLCL xenografts. This tumour rejection was abolished by administration of ganciclovir, which eliminated

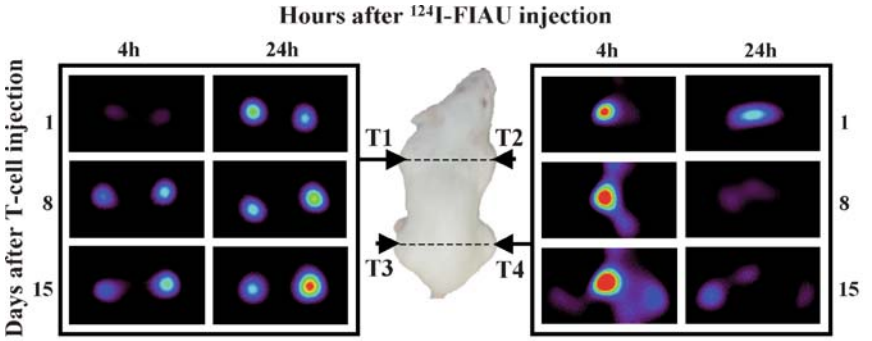

Fig. 15 MicroPET imaging of T-cell migration and targeting. Sequential axial images through the shoulders (*left panel*) and thighs (*right panel*) of mice bearing autologous BLCL ($T1$), HLA-A0201 matched BLCL ($T2$), HLA-mismatched BLCL ($T3$), and HLA-A0201 ALL ($T4$) tumours in the left and right shoulders and the left and right thighs, respectively after i.v injection of [^{124}I]FIAU 1, 8 and 15 days post T-cell infusion. All images are from a single representative animal. (Adapted from Koehne et al. 2003)

the *HSV1-tk*-transduced T-cells (our unpublished data). These studies demonstrate the feasibility of long-term in-vivo monitoring of targeting and migration of antigen-specific CTLs that are transduced to constitutively express a radionuclide-based reporter gene. This paradigm provides the opportunity for repeated visualisation of transferred T-cells within the same animal over time using non-invasive reporter gene PET imaging and it is potentially transferable to clinical studies in patients with EBV+ cancer.

The potential of PET imaging for quantifying cell signals in regions of anatomic interest exists. However, little is known about the constraints and parameters for using PET signal detection to establish cell numbers in different regions of interest. Su et al. (2004) determined the correlation of PET signal to cell number, and characterised the cellular limit of detection for PET imaging. These studies using human T-cells transduced with the *HSV1-tk* reporter gene revealed a cell number-dependent signal, with a limit of detection calculated as 10^6 cells in a region of interest of 0.1 ml volume. Quantitatively similar parameters were observed with stably transduced N2a glioma cells and primary T-lymphocytes.

An essential component of the immune response in many normal and disease states is T-cell activation. Our group has monitored and assessed T-cell receptor (TCR) -dependent activation in vivo using non-invasive PET imaging (Ponomarev et al. 2001). TCR interactions with MHC-peptide complexes expressed on antigen-presenting cells initiate T-cell activation, resulting in transcription that is mediated by several factors. Several of these factors, including IL-2 and other cytokines, contribute to the regulation of a number of target genes through several activating pathways and involve several transcription factors such as nuclear factor of activated T-cells (NFAT) (Li W 1996). Furthermore, this activation can be arrested clinically by the use calcineurin inhibitors such as cyclosporin A and FK506 (Kiani A 2000).

When combined with imaging of NFAT-mediated activation of T-cells, non-invasive PET imaging should allow for monitoring the trafficking, proliferation and antigen-specific activation of T-cells in anti-tumour vaccination trials.

3.3 Imaging the Trafficking of Bone Marrow-derived Cells

Imaging the trafficking of bone marrow-derived cells has also been performed using optical-, MR- and PET-based imaging studies. The use of PET for monitoring bone marrow and progenitor (stem) cell transplantation has lagged behind optical and MR techniques (Kiani et al. 2000; Wang et al. 2003). In most cases, PET imaging has been applied to monitoring bone marrow transplantation (BMT), to assess for residual disease (Hill et al. 2003), or BMT conditioning regimen related toxicities (Vose et al. 1996). Monitoring the fate of bone marrow stem cells with PET following direct labelling with [^{18}F]fluorobenzoate and transplantation was first reported by Olasz et al. (Olasz et al. 2002). Direct labelling of bone marrow-derived cells is limited by the half-life and quantity of isotope used in the labelling. Reporter gene technology precludes this limitation, and allows for extended monitoring of stem cell engraftment (Mayer-Kuckuk et al. 2004). Recently, Cao et al. (2004) reported luciferase bioluminescence imaging of hematopoietic stem cells following transplantation into irradiated recipient mice. Donor stem cells were derived either from a luciferase or luciferase/GFP transgenic mouse and purified through cell sorting. After systemic administration, repeated optical imaging was used to detect the sites and kinetics of hematopoietic stem cell engraftment. The data suggest that the stem cells initially home to the bone marrow or spleen, while little specificity for a particular bone marrow compartment exists. Interestingly, different subsets of progenitor cells, such as short- or long-term repopulating cells, showed comparable homing profiles but differences in their proliferative potential. The potential of bioluminescence imaging to monitor engraftment of hematopoietic progenitor cells was previously shown in a mouse model of xenotransplantation of human hematopoietic stem cell populations (Wang et al. 2003). We have applied reporter gene technology to image the trafficking and distribution of bone marrow cells using a multiple-modality reporter gene approach (Mayer-Kuckuk et al. 2006). Co-registration of microPET and microCT images facilitated interpretation of the PET signal and allowed localisation of radioactive foci to specific anatomical structures (Fig. 16). Others have studied effects of the bone marrow transplanted cells on the reconstruction of the ischemic myocardium (Tomita et al. 2002; Stamm et al. 2003).

3.4 Imaging Oncogenesis and Signalling Pathways in Genetic Modified Mouse Models

Genetic modified mouse models take advantage of the fact that cancer results from mutations in proto-oncogenes and tumour suppressor genes. They allow examination

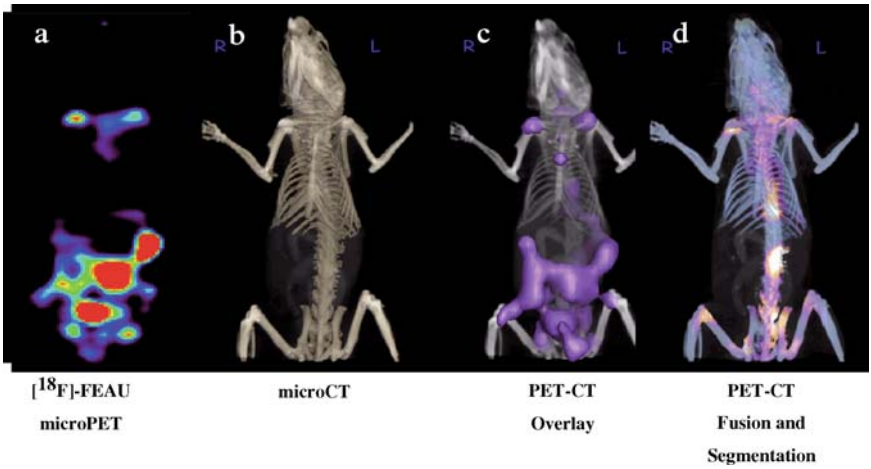

Fig. 16 a–d Multi-modality imaging of autologous bone marrow-derived cells targeting bone. Multi-modality imaging: microPET **a**; microCT **b**; microPET-CT overlay **c**; microPET-CT registration, segmentation and fusion **d**. Bone marrow-derived cells were transduced with a constitutively expressing triple-modality reporter (Ponomarev et al. 2004). The images show targeting of bone and 6 days after i.v. administration. Note that the tomographic display **d** confirms the targeting of transduced cells to bone; a future objective is to perform microPET-MR acquisitions and a similar tomographic microPET-MR registration and fusion to identify soft tissue structures that are targeted or are involved in trafficking of transduced reporter cells. It is also expected that some time in the near future that tomographic bioluminescence and fluorescence images can be obtained, and that these images will be registered with currently available CT, MR and PET tomographic images. [These images were obtained by Philipp Mayer-Kukuck and Debabrata Banerjee, in collaboration with others; the image fusion and segmentation was performed by Dr. Luc Bidault, MSKCC (Mayer-Kuckuk et al. 2006)]

of the consequence of a specific gene alteration on the formation of tumours in their physiological environment. Important for the interpretation of data obtained from mouse models is the ability to accurately detect the consequences that arise from the generated genetic alteration. In most circumstances, onset and temporal dynamics of tumour growth will be a critical assessment. Mouse modelling of cancer (Holland 2004b) and the genetic alterations in mouse models of gliomagenesis have recently been reviewed (Holland 2004a). Since these mouse models require gene manipulation, it is useful to use reporter genes for the non-invasive detection and assessment of tumour growth.

A proof-of-principle study that utilises bioluminescence imaging to detect and measure K-Ras-dependent lung tumour genesis has been reported by Lyons et al. (2003). Mice engineered to induce lung tumours following Cre recombinase-mediated activation of K-Ras over-expression were crossed with animals which provide Cre controlled luciferase expression. Following adenoviral delivery of Cre to the lungs, the formation of multiple lung tumours was observed. Optical bioluminescence imaging using the luciferase reporter gene was capable of monitoring the temporal dynamics of tumour development and progression in the lung of an individual animal (Fig. 17).

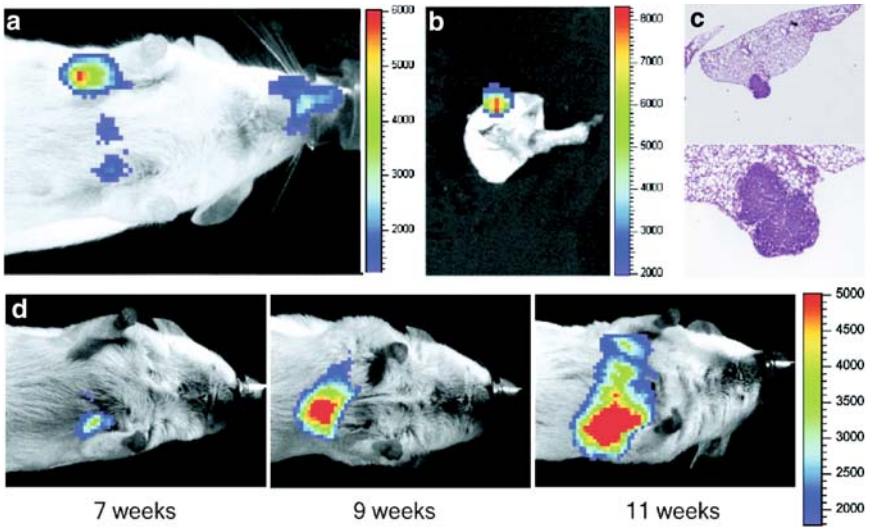

Fig. 17 a–d Bioluminescence imaging of spontaneous lung tumorigenesis and tumour progression. Tumours arising from LucRep/conditional *Kras*2^{v12} mice were visualised non-invasively. **a** IVIS bioluminescence image of a compound LucRep/conditional *Kras*2^{v12} mouse 13 weeks after AdCre intubation shows a bright focal region of luminescence originating from the thorax. **b** IVIS image of the lungs dissected from the mouse depicted in **a** also shows a single origin of light. **c** The same lungs after H&E processing (at ×2.5 and ×10 magnification) showing that the light detected in **a** and **b** originated from a single lesion measuring between 1 and 2 mm in diameter. **d** Longitudinal measurement of *Kras*2^{v12}-induced lung tumour growth in an individual mouse imaged sequentially at 2-week intervals. (Adapted from Lyons et al. 2003)

An important aspect of the report by Lyons et al. (2003) is their methodological approach. Imaging oncogenesis was accomplished by combining a conditional transgenic mouse model of tumour genesis with a conditional transgenic reporter gene mouse. This approach is highly versatile and easily translatable to other mouse models of cancer. However, reporter gene imaging was restricted to monitor tumour development and, therefore, activation of the reporter was only indirectly related to the activation of oncogenic pathways. Furthermore, all non-invasive in-vivo imaging systems have defined limits with respect to image resolution and sensitivity. Hence, it can be anticipated that only established tumours of a minimum size and with an established blood supply can be efficiently monitored by our molecular imaging techniques (e.g. microPET, bioluminescence, fluorescence). It is, therefore, unlikely that the very early events which lead to the formation of cancer can be imaged using some of our currently available molecular imaging techniques, and that further developments in imaging technology will be required to image very small populations of cells. Nevertheless, as described in the next section, reporter gene imaging has a great potential to directly assess the molecular changes that occur during oncogenesis.

The signalling pathways mediated by receptor tyrosine kinase (RTK), including PDGF, EGF and HER2 receptor, are important for oncogenesis and tumour

development. These receptors have been shown to be are frequently mutated, amplified or over-expressed in tumours (Lazar-Molnar et al. 2000; Dai et al. 2001; Holland 2004b; Lyons et al. 2006). RTKs signal through several effector arms, including Ras/MAPK (MAP kinase), PI3K (phosphoinositide 3-kinase), PLC-g (phospholipase C), and JAK-STAT (signal transducers and activators of transcription), which regulate cellular proliferation, migration and invasion, and cytokine stimulation. Furthermore, the PI3K-PKB/Akt signalling pathway plays a critical role in mediating survival signals in a wide range of cell types. The binding of growth factors to specific receptor tyrosine kinases activates the phosphoinositide 3-kinase (PI3K) and the serine-threonine kinase Akt (also called protein kinase B or PKB). Akt has been shown to be activated in many tumours and up-regulation of Akt activity is consistently observed in PTEN-mutant gliomas. Activated forms of Akt substitute for IL-2 signals that phosphorylate Rb and activate E2F during G1 progression (Brennan et al. 1997). Because E2F can up-regulate the expression of c-myc (Moberg et al. 1992; Oswald et al. 1994; Wong et al. 1995), c-myc induction by Akt may be mediated, at least in part, via E2F. In addition, recent experiments suggest that Akt may also use metabolic pathways to regulate cell survival. Given the scope of biological effects from RTK stimulation, it is reasonable to investigate how the dysregulation of these pathways drives malignant transformation, progression and maintenance of these tumours.

Holland et al used the RCAS/TVA system to induce PDGF-driven gliomas in a transgenic mouse model (Dai et al. 2001; Holland 2004b). This system is comprised of two components: (1) an avian retroviral vector referred to as RCAS, (2) an avian tv-a receptor for the RCAS vector (Dai et al. 2001; Sherr and McCormick 2002). They developed an N-tv-a transgenic mouse line, expressing tv-a from the nestin promoter. Infection of RCAS-PDGFB to neural progenitors in N-tv-a mice induced the formation of gliomas in about 60% of mice (Dai et al. 2001) (Fig. 18a).

To monitor the proliferative activity of PDGF-induced gliomas by bioluminescence imaging, they also generated a transgenic reporter mouse using the human E2F1 promoter, which is strictly regulated by RB in cell-cycle progression (Dai et al. 2001; Sherr and McCormick 2002), to drive expression of the firefly luciferase gene (E2F-luc) (Dai et al. 2001; Uhrbom et al. 2004). The E2F-luc transgenic mouse line was then crossbred with the N-tv-a mouse strain. The luciferase activity of PDGF-induced gliomas could be detected in the double transgenic 4 weeks after RCAS-PDGF injection. The time-dependent increase in light production represents the sum of the tumour cells' capacity to proliferate and the overall size of the tumour (Fig. 18a).

3.5 Imaging Drug Treatment in Mouse Tumour Models

A currently applied variant of reporter imaging, particularly in the pharmaceutical industry, is to monitor tumour or xenograft growth using bioluminescence imaging. In this system, the desired cell lines are stably transduced with a luciferase reporter gene that is constitutively expressed. The transduced cells are selected and used to

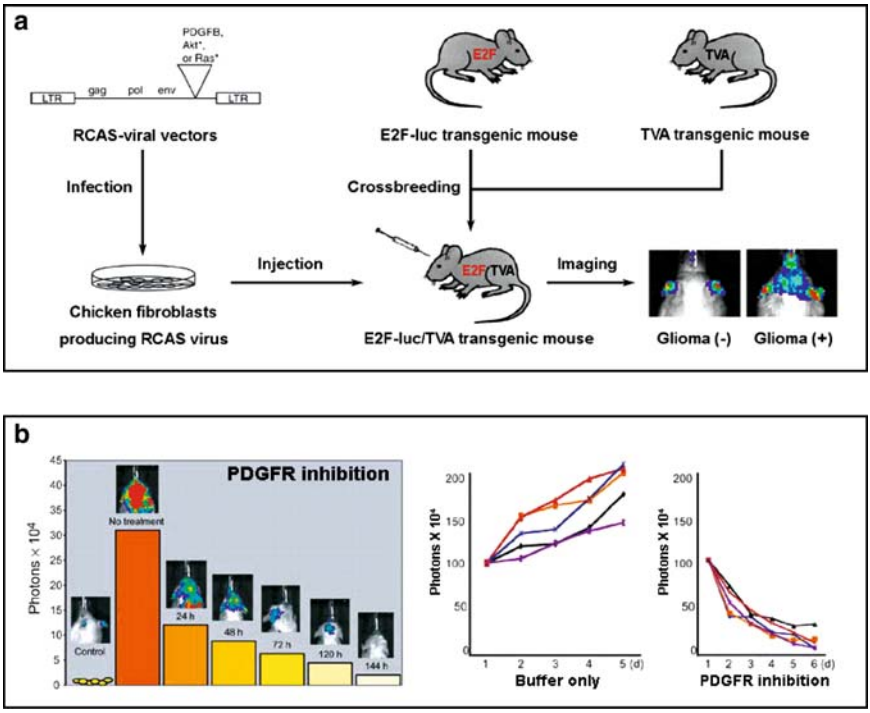

Fig. 18 a, b Bioluminescence imaging of PDGFB-induced glioma in E2F-luc/TVA transgenic mouse model. **a** Generation of PDGFB-induced glioma model in E2F-luc/TVA transgenic mice. PDGFB is inserted into the viral genome, and the modified RCAS virus is propagated in avian cells in vitro. Then the virus-producing cells are injected into the brain of the E2F-luc/TVA double transgenic mice expressing both tv-a (the RCAS receptor) under the nestin promoter and the firefly luciferase under the E2F1 promoter. After 4 weeks of injection, proliferative activity of the induced glioma has been increased and light production has been elevated. **b** Preclinical trials of PDGFB-induced gliomas-bearing E2F-luc/TVA transgenic mouse model. *Left panel:* longitudinal imaging of one tumour-bearing mouse treated with PDGFR inhibitor daily, PTK787/ZK222584, for 6 days. *Middle and right panels:* longitudinal study with five E2F-luc/TVA transgenic mice in each cohort: buffer treated (*middle panel*) or treated daily with PTK787/ZK222584 (*right panel*). (Adapted from Uhrbom et al. 2004)

produce s.c. or orthotopic xenografts. The growth and response to treatment can be monitored effectively in mice by sequential bioluminescence imaging, over time (Rehemtulla et al. 2000) (Fig. 19). The intensity of bioluminescence at a particular site in the animal is directly related to size (number of transduced cells expressing luciferase) of the tumour (Figs. 11, 17,19). The popularity and wide use of bioluminescence reporter imaging is due to its relative simplicity, low cost, high sensitivity and high throughput.

There is a strong rational to assess the effects of drugs that target PDGF/EGFR/HER2 signalling or Ras/Raf/MEK/Erk- and PKB/Akt/mTOR-mediated pathways by non-invasive imaging. The application of biomarker or surrogate imaging using

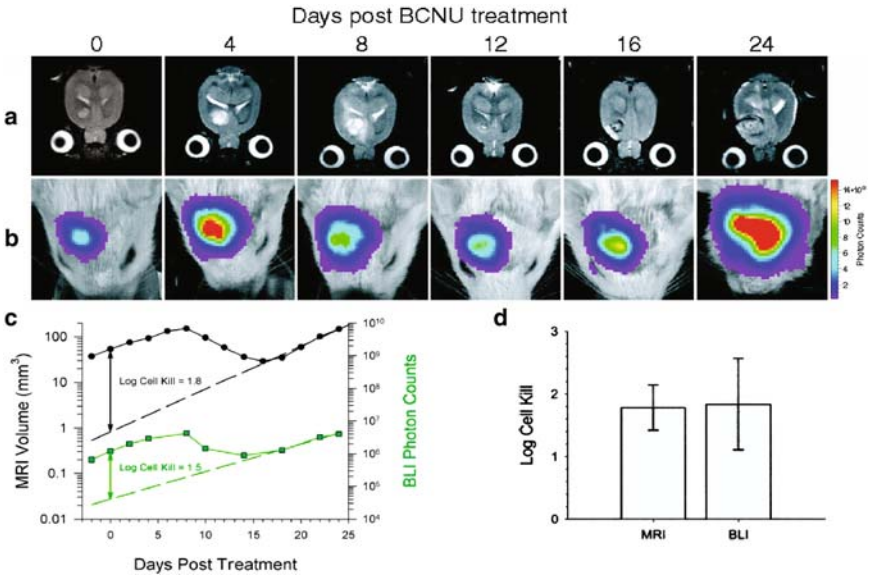

Fig. 19 a–d Temporal analysis of the response of 9LLuc tumour to BCNU chemotherapy. Tumour cells were implanted 16 days before treatment. Tumour volume was monitored with T2-weighted MRI **a** and intra-tumoural luciferase activity was monitored with BLI **b**. The days post-BCNU therapy on which the images were obtained are indicated *at the top*. The *scale to the right* of the BL images describes the colour map for the photo count. **c** Quantitative analysis of tumour progression and response to BCNU treatment. Tumour volumes and total tumour photon emission obtained by T2-weighted MRI and BLI, respectively, are plotted versus days post-BCNU treatment. The *dashed lines* are the regression fits of exponential tumour repopulation following therapy. The *solid vertical lines* denote the apparent tumour-volume and photon-production losses elicited by BCNU on the day of treatment from which log cell-kill values were calculated as previously described (Nakagawa et al. 2001). **d** Comparison of log cell-kill values determined from MRI and BLI measurements. Log cell-kill elicited by BCNU chemotherapy was calculated using MRI $(1.78 + 0.36)$ and BLI $(1.84 + 0.73)$. Data are represented as mean + SEM for each animal $(n = 5)$. There was no statistically significant difference between the log kills calculated using the MRI abd BLI data $(P = 0.951)$. (Adapted from Rehemtulla et al. 2000)

FDG and PET has been discussed above. The development and use of reporter- and direct-imaging paradigms to evaluate the efficacy of molecular-targeted therapies is now being pursued by many groups. Specific drugs that are known (or thought) to target specific signalling pathways and down-stream effectors can be assessed in the reporter-xenografts or transgenic/oncogenic reporter-animals. Namely, the effects of treatment targeted to a particular signalling pathway can be assessed by non-invasive imaging.

For example, the E2F-reporter mouse model, that monitors the proliferative activity, was used by the Holland laboratory in longitudinal preclinical studies to study the effects of treatment with a drug, PTK787/ZK222584, that inhibits the PDGF receptor. Compared with the buffer-treated control group animals, mice treated with PTK787/ZK222584 showed a clear reduction in light emission from the brain area

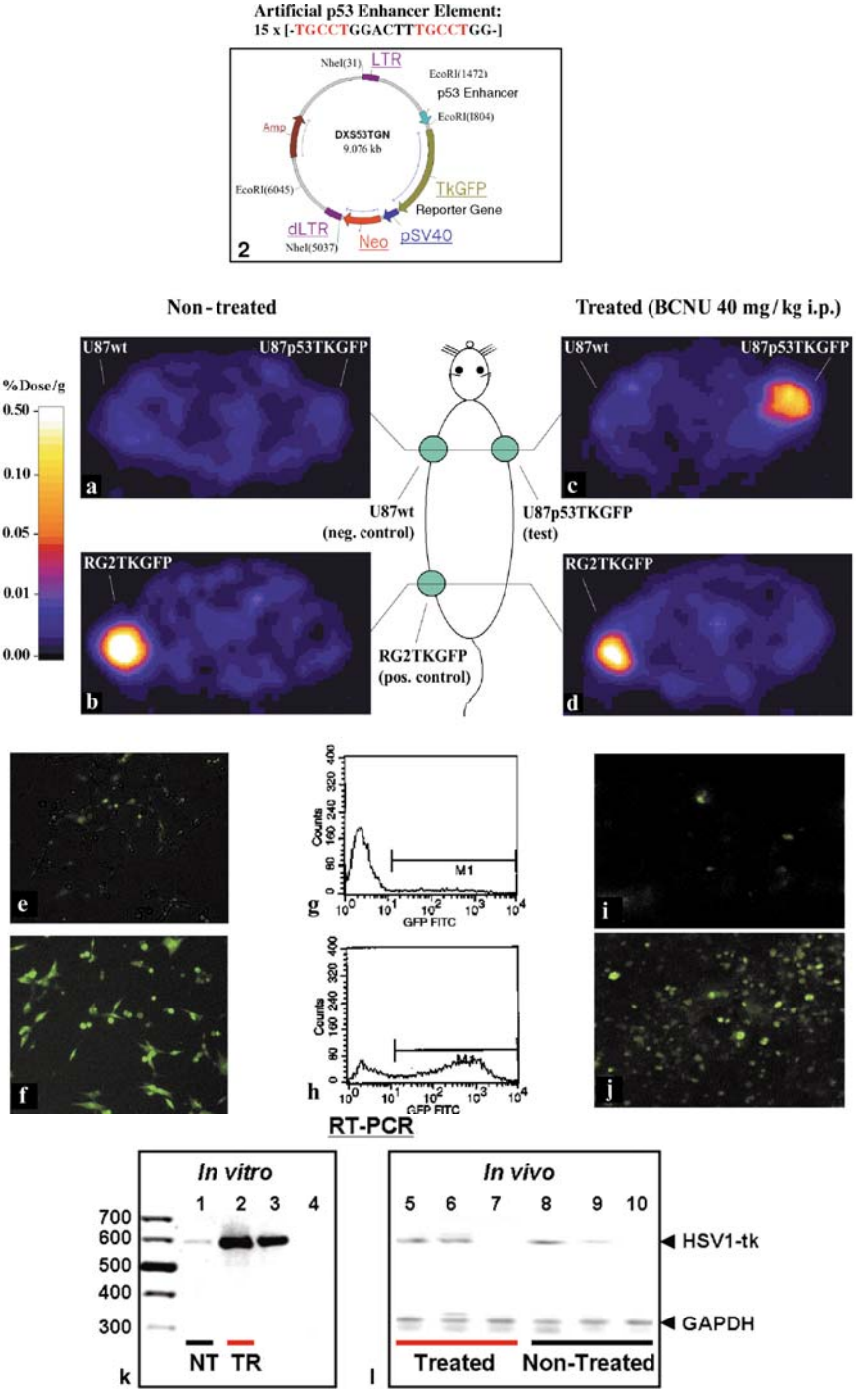
Artificial p53 Enhancer Element:
15 x [-TGCCTGGACTTTGCCTGG-]
NheI(31)
LTR
EcoRI(1472)
p53 Enhancer
EcoRI(1804)
Amp
DXS53TGN
9.076 kb
EcoRI(6045)
TkGFP
Reporter Gene
dLTR
NheI(5037)
Neo
pSV40
2
Non-treated
Treated (BCNU 40 mg/kg i.p.)
%Dose/g
0.50
0.10
0.05
0.01
0.00
U87wt
U87p53TKGFP
a
c
U87wt
(neg. control)
U87p53TKGFP
(test)
RG2TKGFP
b
d
RG2TKGFP
(pos. control)
e
f
g
h
i
j
Counts
M1
GFP FITC
RT-PCR
In vitro
In vivo
1 2 3 4
5 6 7 8 9 10
700
600
500
400
300
HSV1-tk
GAPDH
NT TR
Treated
Non-Treated
k
l

Fig. 20 a–l Imaging BCNU activation of p53. The p53-sensitive, dual-modality reporter vector (*top panel*) contains an artificial p53 specific enhancer element that activates expression of the *HSV1-TK/eGFP* reporter gene. A constitutively expressed neomycin selection gene is also included in the retroviral vector construct. Transaxial PET images (GE Advance tomograph) through the shoulder **a, c** and pelvis **b, d** of two rats are shown (*second panel*); the images are colour-coded to the same radioactivity scale (*% dose/g*). An untreated animal is shown on the *left* **a, b**, and a BCNU-treated animal, which is known to activate the p53 pathway, is shown on the *right* **c, d**. Both animals have three s.c. xenografts: a U87p53TKGFP (*test*) in the right shoulder, a U87 wild-type (*negative control*) in the left shoulder, and a RG2TKGFP (*positive control*) in the left thigh. The non-treated animal on the left shows localisation of radioactivity only in the positive control tumour (*RG2TKGFP*); the test (*U87p53TKGFP*) and negative control (*U87wt*) xenografts are at background levels. The BCNU-treated animal on the right shows significant radioactivity localisation in the test tumour (right shoulder) and in the positive control (left thigh), but no radioactivity above background in the negative control (left shoulder). Fluorescence microscopy and FACS analysis (*third panel*) of a transduced U87p53/TKGFP cell population in the non-induced (control) state **e, g**, and 24 h after a 2-h treatment with BCNU 40 mg/ml **f, h** are shown. Fluorescence microscopic images of post-motem U87p53/TKGFP s.c. tumour samples obtained from non-treated rats **i** and rats treated with 40 mg/kg BCNU i.p. **j** are also shown. These results **f–j** demonstrate a corresponding activation of the reporter system (increased fluorescence) due to p53 induction by BCNU treatment. RT-PCR blots from in-vitro **k** and in-vivo **l** experiments (*lower panel*) show very low HSV1-tk expression in non-treated U87p53TKGFP transduced cells and xenografts-bearing animals, respectively, and no HSV1-tk expression in wild-type U87 cells and tumour tissue, respectively. When U87p53TKGFP transduced cells and xenografts-bearing animals are treated with BCNU, there is a marked increase in HSV1-tk expression, comparable to that in constitutively HSV1-tk-expressing RG2TK$^+$ cells and xenografts. (Adapted from Doubrovin et al. 2001)

over 5 days (Fig. 18b). The reduction in light production was also found to be proportional to the cell proliferation index. The E2F-reporter mouse model makes it possible to investigate the importance of PDGF-related signalling pathways in glioma maintenance. The non-invasive imaging allows for dynamic in-vivo monitoring of a specific signal transduction pathway activity and precludes the animal euthanasia that is usually required to obtain tissue samples for molecular assays. It is also a valuable tool to obtain the more accurate and detailed measurement of biological processes during tumour treatment by the pathway specific/targeting drugs. Based on the strategy of construction of reporter-bearing mouse model, the activation of a specific oncogene during tumorigenesis has also been monitored through an oncogene promoter that controls the expression of a reporter gene. For example, the PSA-luc reporter mouse was used in prostate cancer model (Dai et al. 2001; Lyons et al. 2006), and the pVEGF-TSTA-luc reporter mouse was constructed for mammary tumorigenesis model (Wang et al. 2006).

As discussed above, and this has been developed and validated for several transcriptional-sensitive reporter systems (Doubrovin et al. 2001; Serganova et al. 2004). Up-regulation of these transcription factors was demonstrated and correlated with the expression of downstream-dependent genes [e.g. p21, vascular endothelial growth factor (VEGF), respectively]. Imaging BCNU activation of p53 is shown in Fig. 20. Such assays can be applied to tumours or xenografts that have been transduced with the appropriate reporter construct, or in appropriate transgenic reporter-animal models of cancer.

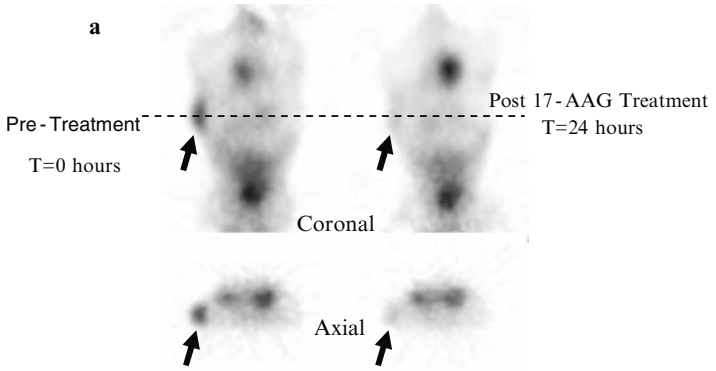

Fig. 21 a–c Monitoring the effect of 17-AAG on tumour HER2 expression. **a** Coronal and transaxial MicroPET images of $[^{68}Ga]$-F$(ab)_2$-Herceptin in a single nude mouse bearing a single BT 474 xenograft (*arrow*). Both image sets were acquired 3 h after i.v. injection of approximately 5 MBq of $[^{68}Ga]$-F$(ab)_2$-herceptin. The pre-treatment images are shown on the *left*; the post-treatment images are shown on the *right*. Treatment involved 17-AAG administered 3×50 mg/kg over 24 h, followed by imaging 24 h later. **b** The pharmacodynamics and pharmacokinetcs of HER2 expression levels following two different 17-AAG treatment schedules. MicroPET determinations of average HER2 expression in two groups of mice $(n = 5)$ over a 1-week period. One treatment group (a) of mice received 2×100 mg/kg 17-AAG over 24 h, and the other treatment group (b) received 3×50 mg/kg 17-AAG over 24 h after the initial microPET scan; the control animals in each group received vehicle only. The data are normalised to the initial pretreatment uptake value. A significant difference in treatment effect on HER2 expression levels is seen between the two schedules of 17-AAG administration. **c** Western blot analysis of HER2 and the 85-kDa regulatory subunit of P13 kinase expression in BT-474 tumours from control mice and from mice 24 H treatment with 17-AAG. (Adapted from Smith-Jones et al. 2004)

In a recent study, imaging was used to sequentially monitor the pharmacodynamics of HER2 degradation in response to treatment with a HER2-chaperone protein (HSP90) inhibitor (17-AAG) (Smith-Jones et al. 2004). This study demonstrates that a highly specific, small $F(ab')_2$ antibody fragment can be diolabeled with a short-lived nuclide and used for repetitive non-invasive imaging of HER2 degradation and recovery (Fig. 21). What was novel in this study was the ability to image the target of therapy, HER2, through the effects of a drug on the HER2 chaperone protein (HSP90) rather than through an inhibition of HER2 function. The ansamycin class of antibiotics, including geldanamycin and its derivative 17-AAG, bind to the ATP-binding pocket of HSP90 and inhibit its chaperone function. The HSP90 chaperone is required for conformational maturation and stability of a number of key signalling molecules, including HER2, AKT, RAF, cdk4 serine kinases, and results in their proteosomal degradation (Neckers 2002). Since HER2 is dependent on HSP90 and is particularly sensitive to 17-AAG treatment, Smith-Jones et al. (2004) exploited this mechanism of action to image the pharmacodynamic effects of 17-AAG on HER2 (through the drug's effect on the chaperone protein) (Fig. 21). This approach could be extended to other targets of drug therapy, such as MET, IGF-1 and other RTKs that are HSP90 chaperone-dependent and could easily be adapted to human studies to provide the opportunity to non-invasively image the pharmacodynamics of drug action by repetitive imaging over time using short-lived radionuclides. The ability to image drug pharmacodynamic effects addresses a major impediment to the development of rational therapeutic strategies; namely, the determination of whether the drug treatment protocol (dose and schedule) is actually inhibiting the target and whether the level of inhibition is sufficient. Furthermore, it is not inconceivable that non-invasive imaging of drug pharmacodynamic effects could be applied to individual patients, in order to optimise dose and administration schedule.

4 Conclusions

Molecular genetic studies of disease and our understanding of the multiple and converging pathways that are involved in disease development (e.g. oncogenesis and tumour progression) have expanded rapidly over the past decade. The era of molecular medicine has begun and the benefits to individual patients are widely expected to be realised in the near future. For example, the formerly unresponsive and rapidly fatal gastrointestinal stromal tumours (GIST) and chronic myelogenous leukemia (CML) have shown remarkable responses to imatinib mesylate (Gleevac) treatment, a drug that targets several receptor tyrosine kinases (cKit and Bcr-Abl, respectively) that are mutated or constitutively over-expressed.

Biomarker or surrogate imaging that reflects endogenous molecular/genetic processes is particularly attractive for expansion and translation into clinical studies in the short-term. This is because existing radiopharmaceuticals and imaging paradigms may be useful for monitoring down-stream changes of specific molecular/genetic pathways in diseases such as cancer (e.g. FDG PET). Biomarker imaging

is very likely to be less specific and more limited with respect to the number of molecular genetic processes that can be imaged. Nevertheless, it benefits from the use of radiopharmaceuticals that have already been developed and are currently being used in human subjects. Thus, the translation and application of biomarker imaging paradigms into patient studies will be far easier than either the direct imaging or reporter transgene imaging paradigms.

The "direct" molecular imaging motif builds on established chemistry and radiochemistry relationships. Bioconjugate chemistry linking specific binding motifs and bioactive molecules to paramagnetic particles for MR imaging or to radionuclides for PET and gamma camera imaging is rapidly expanding. This has occurred largely through the development of new relationships and focused interactions between molecular/cellular biologists, chemists, radiochemists, imagers and clinicians. The next generation of direct molecular imaging probes will come from better interactions between pharmaceutical companies, academia and hospitals. Such interactions are now being pursued with the objective to develop and evaluate new compounds for imaging; compounds that target specific molecules (e.g. DNA, mRNA, proteins) or activated enzyme systems in specific signal transduction pathways. However, a constraint limiting direct imaging strategies is the necessity to develop a specific probe for each molecular target, and then to validate the sensitivity, specificity and safety of each probe for specific applications prior to their introduction into the clinic.

Reporter gene imaging studies will be more limited in patients compared with that in animals, due to the necessity of transducing the target tissue or cells with specific reporter constructs, or the production of transgenic animals bearing the reporter constructs. Ideal vectors for targeting specific organs or tissue (tumours) do not exist at this time, although this is a very active area of human gene therapy research. Each new vector requires extensive and time-consuming safety testing prior to regulatory approval for human administration. Nevertheless, the reporter gene imaging, particularly the genetic labelling of cells with reporter constructs, has several advantages. For example, it is possible to develop and validate "indirect" imaging strategies more rapidly and at considerably lower cost than "direct" imaging strategies. This is because only a small number of well characterised and validated reporter gene-reporter probe pairs need to be established. For example, there are now four well-defined human genes (*hNIS, hNET, hD2R* and *hSSTR2*) with complimentary, clinically approved, radiopharmaceuticals for PET or gamma-camera imaging in patients. These four complimentary pairs (gene + probe) are excellent candidates for future reporter gene imaging in patients. Importantly, these human genes are less likely to be immunogenic compared with the reporter genes currently used in animals (e.g. viral thymidine kinases, luciferases, fluorescent proteins). It should also be noted that a single reporter gene-reporter probe pair can be used in different reporter constructs to image many different biological and molecular genetic processes. Once a complimentary reporter-pair (gene + probe) has been approved for human studies, the major regulatory focus will shift to the particular backbone and regulatory sequence of the reporter construct and to the vector used to target reporter transduction to specific cells or tissue, both ex vivo and in vivo.

The major factor limiting translation of reporter gene imaging studies to patients is the "transduction requirement"; target tissue or adoptively administered cells must be transduced (usually with viral vectors to achieve high transduction efficiency) with reporter constructs for reporter gene imaging studies. At least *two* different reporter constructs will be required in most future applications of reporter gene imaging. One will be a "constitutive" reporter that will be used to identify the site, extent and duration of vector delivery and tissue transduction or for identifying the distribution/trafficking, homing/targeting and persistence of adoptively administered cells (the "normalising" or denominator term). The second one will be an "inducible" reporter that is sensitive to endogenous transcription factors, signalling pathways or protein-protein interactions that monitor the biological activity and function of the transduced cells (the "sensor" or numerator term). The initial application of such double-reporter systems in patients will most likely be performed as part of a gene therapy protocol or an adoptive therapy protocol where the patients own cells are harvested (e.g. lymphocytes, T-cells or blood-derived progenitor cells), transduced with the reporter systems and expanded ex vivo, and then adoptively re-administered to the patient. For example, adoptive T-cell therapy could provide a venue for imaging T-cell trafficking, targeting, activation, proliferation and persistence. These issues could be addressed in a quantitative manner by repetitive PET imaging of the double-reporter system described above in the same subject over time.

We remain optimistic; the tools and resources largely exist and we should be able to perform limited gene imaging studies in patients in the near future. The advantages and benefits of non-invasive imaging to monitor transgene expression in gene therapy protocols are obvious. The ability to visualise transcriptional and post-transcriptional regulation of endogenous target gene expression, as well as specific intracellular protein-protein interactions in patients will provide the opportunity for new experimental venues in patients. They include the potential to image the malignant phenotype of an individual patient's tumour at a molecular level and to monitor changes in the phenotype over time. The potential to image a drug's effect on a specific signal transduction pathway in an individual patient's tumour provides the opportunity for monitoring treatment response at the molecular level. At the moment this requires the use of "diagnostic" reporter gene transduction vectors that target specific organs or tissue (tumours), and this will initially limit the translation and application of reporter gene technology to patients. However, direct and surrogate molecular imaging may begin to fill this gap over the next decade.

References

Adonai N NK, Walsh J, Iyer M, Toyokuni T, Phelps ME, McCarthy T, McCarthy DW, Gambhir SS (2002) Ex vivo cell labeling with 64Cu-pyruvaldehyde-bis(N4-methylthiosemicarbazone) for imaging cell trafficking in mice with positron-emission tomography. Proc Natl Acad Sci USA 99:3030–3035

Alauddin MM, Conti PS (1998) Synthesis and preliminary evaluation of 9-(4-[18F]-fluoro-3-hydroxymethylbutyl)guanine ([18F]FHBG): a new potential imaging agent for viral infection and gene therapy using PET. Nucl Med Biol 25:175–180

Altmann A, Kissel M, Zitzmann S, Kubler W, Mahmut M, Peschke P, Haberkorn U (2003) Increased MIBG uptake after transfer of the human norepinephrine transporter gene in rat hepatoma. J Nucl Med 44:973–980

Arbab AS, Yocum GT, Rad AM, Khakoo AY, Fellowes V, Read EJ, Frank JA (2005) Labeling of cells with ferumoxides-protamine sulfate complexes does not inhibit function or differentiation capacity of hematopoietic or mesenchymal stem cells. NMR Biomed 18:553–559

Arbab AS, Yocum GT, Kalish H, Jordan EK, Anderson SA, Khakoo AY, Read EJ, Frank JA (2004) Efficient magnetic cell labeling with protamine sulfate complexed to ferumoxides for cellular MRI. Blood 104:1217–1223

Artemov D, Mori N, Ravi R, Bhujwalla ZM (2003) Magnetic resonance molecular imaging of the HER-2/neu receptor. Cancer Res 63:2723–2727

Bachtiary B, Schindl M, Potter R, Dreier B, Knocke TH, Hainfellner JA, Horvat R, Birner P (2003) Overexpression of hypoxia-inducible factor 1alpha indicates diminished response to radiotherapy and unfavorable prognosis in patients receiving radical radiotherapy for cervical cancer. Clin Cancer Res 9:2234–2240

Berger F, Gambhir SS (2001) Recent advances in imaging endogenous or transferred gene expression utilizing radionuclide technologies in living subjects: applications to breast cancer. Breast Cancer Res 3:28–35

Bhaumik S, Gambhir SS (2002) Optical imaging of Renilla luciferase reporter gene expression in living mice. Proc Natl Acad Sci USA 99:377–382

Blasberg RG, Gelovani J (2002) Molecular-genetic imaging: a nuclear medicine-based perspective. Mol Imaging 1:280–300

Blasberg RG, Tjuvajev JG (2003) Molecular-genetic imaging: current and future perspectives. J Clin Invest 111:1620–1629

Blend MJ, Stastny JJ, Swanson SM, Brechbiel MW (2003) Labeling anti-HER2/neu monoclonal antibodies with 111In and 90Y using a bifunctional DTPA chelating agent. Cancer Biother Radiopharm 18:355–363

Boland A, Ricard M, Opolon P, Bidart JM, Yeh P, Filetti S, Schlumberger M, Perricaudet M (2000) Adenovirus-mediated transfer of the thyroid sodium/iodide symporter gene into tumors for a targeted radiotherapy. Cancer Res 60:3484–3492

Bradley J, Thorstad WL, Mutic S, Miller TR, Dehdashti F, Siegel BA, Bosch W, Bertrand RJ (2004) Impact of FDG-PET on radiation therapy volume delineation in non-small-cell lung cancer. Int J Radiat Oncol Biol Phys 59:78–86

Brennan P, Babbage JW, Burgering BM, Groner B, Reif K, Cantrell DA (1997) Phosphatidylinositol 3-kinase couples the interleukin-2 receptor to the cell cycle regulator E2F. Immunity 7:679–689

Brizel DM, Scully SP, Harrelson JM, Layfield LJ, Bean JM, Prosnitz LR, Dewhirst MW (1996) Tumor oxygenation predicts for the likelihood of distant metastases in human soft tissue sarcoma. Cancer Res 56:941–943

Brown RS, Leung JY, Fisher SJ, Frey KA, Ethier SP, Wahl RL (1996) Intratumoral distribution of tritiated-FDG in breast carcinoma: correlation between Glut-1 expression and FDG uptake. J Nucl Med 37:1042–1047

Brun NC, Moen A, Borch K, Saugstad OD, Greisen G (1997) Near-infrared monitoring of cerebral tissue oxygen saturation and blood volume in newborn piglets. Am J Physiol 273:H682–H686

Bulte JW, Arbab AS, Douglas T, Frank JA (2004) Preparation of magnetically labeled cells for cell tracking by magnetic resonance imaging. Methods Enzymol 386:275–299

Cammilleri S, Sangrajrang S, Perdereau B, Brixy F, Calvo F, Bazin H, Magdelenat H (1996) Biodistribution of iodine-125 tyramine transforming growth factor alpha antisense oligonucleotide in athymic mice with a human mammary tumour xenograft following intratumoral injection. Eur J Nucl Med 23:448–452

Campbell RE, Tour O, Palmer AE, Steinbach PA, Baird GS, Zacharias DA, Tsien RY (2002) A monomeric red fluorescent protein. Proc Natl Acad Sci USA 99:7877–7882

Cao YA, Wagers AJ, Beilhack A, Dusich J, Bachmann MH, Negrin RS, Weissman IL, Contag CH (2004) Shifting foci of hematopoiesis during reconstitution from single stem cells. Proc Natl Acad Sci USA 101:221–226

Chapman JD, Baer K, Lee J (1983) Characteristics of the metabolism-induced binding of misonidazole to hypoxic mammalian cells. Cancer Res 43:1523–1528

Che J, Doubrovin M, Serganova I, Ageyeva L, Zanzonico P, Blasberg R (2005) hNIS-IRES-eGFP dual reporter gene imaging. Mol Imaging 4:128–136

Chievitz O and Hevesy G (1935) Radioactive indicators in the study of phosphorous metabolism in rats. Nature 136:754–755

Chishima T, Miyagi Y, Wang X, Yamaoka H, Shimada H, Moossa AR, Hoffman RM (1997) Cancer invasion and micrometastasis visualized in live tissue by green fluorescent protein expression. Cancer Res 57:2042–2047

Chudakov DM, Verkhusha VV, Staroverov DB, Souslova EA, Lukyanov S, Lukyanov KA (2004) Photoswitchable cyan fluorescent protein for protein tracking. Nat Biotechnol 22:1435–1439

Colpaert CG, Vermeulen PB, Fox SB, Harris AL, Dirix LY, Van Marck EA (2003) The presence of a fibrotic focus in invasive breast carcinoma correlates with the expression of carbonic anhydrase IX and is a marker of hypoxia and poor prognosis. Breast Cancer Res Treat 81:137–147

Contag CH, Spilman SD, Contag PR, Oshiro M, Eames B, Dennery P, Stevenson DK, Benaron DA (1997) Visualizing gene expression in living mammals using a bioluminescent reporter. Photochem Photobiol 66:523–531

Contag PR, Olomu IN, Stevenson DK, Contag CH (1998) Bioluminescent indicators in living mammals. Nat Med 4:245–247

Contag CH, Ross BD (2002) It's not just about anatomy: in vivo bioluminescence imaging as an eyepiece into biology. J Magn Reson Imaging 16:378–387

Cooper R, Sarioglu S, Sokmen S, Fuzun M, Kupelioglu A, Valentine H, Gorken IB, Airley R, West C (2003) Glucose transporter-1 (GLUT-1): a potential marker of prognosis in rectal carcinoma? Br J Cancer 89:870–876

Costa GL SM, Nakajima A, Nguyen EV, Taylor-Edwards C, Slavin AJ, Contag CH, Fathman CG, Benson JM (2001) Adoptive immunotherapy of experimental autoimmune encephalomyelitis via T cell delivery of the IL-12 p40 subunit. J Immunol 167:2379–2387

Dai C, Celestino JC, Okada Y, Louis DN, Fuller GN, Holland EC (2001) PDGF autocrine stimulation dedifferentiates cultured astrocytes and induces oligodendrogliomas and oligoastrocytomas from neural progenitors and astrocytes in vivo. Genes Dev 15:1913–1925

Dai G, Levy O, Carrasco N (1996) Cloning and characterization of the thyroid iodide transporter. Nature 379:458–460

Dehdashti F, Mortimer JE, Siegel BA, Griffeth LK, Bonasera TJ, Fusselman MJ, Detert DD, Cutler PD, Katzenellenbogen JA, Welch MJ (1995) Positron tomographic assessment of estrogen receptors in breast cancer: comparison with FDG-PET and in vitro receptor assays. J Nucl Med 36:1766–1774

Demetri GD, von Mehren M, Blanke CD, Van den Abbeele AD, Eisenberg B, Roberts PJ, Heinrich MC, Tuveson DA, Singer S, Janicek M, Fletcher JA, Silverman SG, Silberman SL, Capdeville R, Kiese B, Peng B, Dimitrijevic S, Druker BJ, Corless C, Fletcher CD, Joensuu H (2002) Efficacy and safety of imatinib mesylate in advanced gastrointestinal stromal tumors. N Engl J Med 347:472–480

Dewanjee MK, Ghafouripour AK, Kapadvanjwala M, Dewanjee S, Serafini AN, Lopez DM, Sfakianakis GN (1994) Noninvasive imaging of c-myc oncogene messenger RNA with indium-111-antisense probes in a mammary tumor-bearing mouse model. J Nucl Med 35:1054–1063

Di Chiro G, DeLaPaz RL, Brooks RA, Sokoloff L, Kornblith PL, Smith BH, Patronas NJ, Kufta CV, Kessler RM, Johnston GS, Manning RG, Wolf AP (1982) Glucose utilization of cerebral gliomas measured by [18F] fluorodeoxyglucose and positron emission tomography. Neurology 32:1323–1329

Dodd CH, Hsu HC, Chu WJ, Yang P, Zhang HG, Mountz JD Jr, Zinn K, Forder J, Josephson L, Weissleder R, Mountz JM, Mountz JD (2001) Normal T-cell response and in vivo magnetic resonance imaging of T cells loaded with HIV transactivator-peptide-derived superparamagnetic nanoparticles. J Immunol Methods 256:89–105

Doubrovin M, Ponomarev V, Beresten T, Balatoni J, Bornmann W, Finn R, Humm J, Larson S, Sadelain M, Blasberg R, Gelovani Tjuvajev J (2001) Imaging transcriptional regulation of p53-dependent genes with positron emission tomography in vivo. Proc Natl Acad Sci USA 98:9300–9305

Druker BJ, Tamura S, Buchdunger E, Ohno S, Segal GM, Fanning S, Zimmermann J, Lydon NB (1996) Effects of a selective inhibitor of the Abl tyrosine kinase on the growth of Bcr-Abl positive cells. Nat Med 2:561–566

Edinger M, Cao YA, Hornig YS, Jenkins DE, Verneris MR, Bachmann MH, Negrin RS, Contag CH (2002) Advancing animal models of neoplasia through in vivo bioluminescence imaging. Eur J Cancer 38:2128–2136

Elas M, Williams BB, Parasca A, Mailer C, Pelizzari CA, Lewis MA, River JN, Karczmar GS, Barth ED, Halpern HJ (2003) Quantitative tumor oxymetric images from 4D electron paramagnetic resonance imaging (EPRI): methodology and comparison with blood oxygen level-dependent (BOLD) MRI. Magn Reson Med 49:682–691

Ellenberg J, Lippincott-Schwartz J, Presley JF (1999) Dual-colour imaging with GFP variants. Trends Cell Biol 9:52–56

Evans SM, Kachur AV, Shiue CY, Hustinx R, Jenkins WT, Shive GG, Karp JS, Alavi A, Lord EM, Dolbier WR, Jr., Koch CJ (2000) Noninvasive detection of tumor hypoxia using the 2-nitroimidazole [18F]EF1. J Nucl Med 41:327–336

Evans SM, Judy KD, Dunphy I, Jenkins WT, Nelson PT, Collins R, Wileyto EP, Jenkins K, Hahn SM, Stevens CW, Judkins AR, Phillips P, Geoerger B, Koch CJ (2004) Comparative measurements of hypoxia in human brain tumors using needle electrodes and EF5 binding. Cancer Res 64:1886–1892

Falk MM, Lauf U (2001) High resolution, fluorescence deconvolution microscopy and tagging with the autofluorescent tracers CFP, GFP, and YFP to study the structural composition of gap junctions in living cells. Microsc Res Tech 52:251–262

Forss-Petter S, Danielson PE, Catsicas S, Battenberg E, Price J, Nerenberg M, Sutcliffe JG (1990) Transgenic mice expressing beta-galactosidase in mature neurons under neuron-specific enolase promoter control. Neuron 5:187–197

Frauwirth KA, Riley JL, Harris MH, Parry RV, Rathmell JC, Plas DR, Elstrom RL, June CH, Thompson CB (2002) The CD28 signaling pathway regulates glucose metabolism. Immunity 16:769–777

Funovics MA, Kapeller B, Hoeller C, Su HS, Kunstfeld R, Puig S, Macfelda K (2004) MR imaging of the her2/neu and 9.2.27 tumor antigens using immunospecific contrast agents. Magn Reson Imaging 22:843–850

Fyfe JA, Keller PM, Furman PA, Miller RL, Elion GB (1978) Thymidine kinase from herpes simplex virus phosphorylates the new antiviral compound, 9-(2-hydroxyethoxymethyl)guanine. J Biol Chem 253:8721–8727

Gallardo HF, Tan C, Ory D, Sadelain M (1997) Recombinant retroviruses pseudotyped with the vesicular stomatitis virus G glycoprotein mediate both stable gene transfer and pseudotransduction in human peripheral blood lymphocytes. Blood 90:952–957

Gambhir SS (2002) Molecular imaging of cancer with positron emission tomography. Nat Rev Cancer 2:683–693

Gambhir SS, Barrio JR, Wu L, Iyer M, Namavari M, Satyamurthy N, Bauer E, Parrish C, MacLaren DC, Borghei AR, Green LA, Sharfstein S, Berk AJ, Cherry SR, Phelps ME, Herschman HR (1998) Imaging of adenoviral-directed herpes simplex virus type 1 thymidine kinase reporter gene expression in mice with radiolabeled ganciclovir. J Nucl Med 39:2003–2011

Gambhir SS, Barrio JR, Phelps ME, Iyer M, Namavari M, Satyamurthy N, Wu L, Green LA, Bauer E, MacLaren DC, Nguyen K, Berk AJ, Cherry SR, Herschman HR (1999) Imaging adenoviral-directed reporter gene expression in living animals with positron emission tomography. Proc Natl Acad Sci USA 96:2333–2338

Gambhir SS, Bauer E, Black ME, Liang Q, Kokoris MS, Barrio JR, Iyer M, Namavari M, Phelps ME, Herschman HR (2000a) A mutant herpes simplex virus type 1 thymidine kinase reporter gene shows improved sensitivity for imaging reporter gene expression with positron emission tomography. Proc Natl Acad Sci USA 97:2785–2790

Gambhir SS, Herschman HR, Cherry SR, Barrio JR, Satyamurthy N, Toyokuni T, Phelps ME, Larson SM, Balatoni J, Finn R, Sadelain M, Tjuvajev J, Blasberg R (2000b) Imaging transgene expression with radionuclide imaging technologies. Neoplasia 2:118–138

Gelovani Tjuvajev J, Blasberg RG (2003) In vivo imaging of molecular-genetic targets for cancer therapy. Cancer Cell 3:327–332

Giatromanolaki A, Koukourakis MI, Sivridis E, Pastorek J, Wykoff CC, Gatter KC, Harris AL (2001) Expression of hypoxia-inducible carbonic anhydrase-9 relates to angiogenic pathways and independently to poor outcome in non-small cell lung cancer. Cancer Res 61:7992–7998

Gillies RJ, Raghunand N, Karczmar GS, Bhujwalla ZM (2002) MRI of the tumor microenvironment. J Magn Reson Imaging 16:430–450

Gobuty AH RR, Barth RF (1977) Organ distribution of 99mTc- and 51Cr-labeled autologous peripheral blood lymphocytes in rabbits. J Nucl Med 18: 141–146

Green LA, Yap CS, Nguyen K, Barrio JR, Namavari M, Satyamurthy N, Phelps ME, Sandgren EP, Herschman HR, Gambhir SS (2002) Indirect monitoring of endogenous gene expression by positron emission tomography (PET) imaging of reporter gene expression in transgenic mice. Mol Imaging Biol 4:71–81

Gupta AK, Hutchinson PJ, Fryer T, Al-Rawi PG, Parry DA, Minhas PS, Kett-White R, Kirkpatrick PJ, Mathews JC, Downey S, Aigbirhio F, Clark J, Pickard JD, Menon DK (2002) Measurement of brain tissue oxygenation performed using positron emission tomography scanning to validate a novel monitoring method. J Neurosurg 96:263–268

Gurskaya NG, Fradkov AF, Terskikh A, Matz MV, Labas YA, Martynov VI, Yanushevich YG, Lukyanov KA, Lukyanov SA (2001) GFP-like chromoproteins as a source of far-red fluorescent proteins. FEBS Lett 507:16–20

Haberkorn U (2001) Gene therapy with sodium/iodide symporter in hepatocarcinoma. Exp Clin Endocrinol Diabetes 109:60–62

Hadjantonakis AK, Nagy A (2001) The color of mice: in the light of GFP-variant reporters. Histochem Cell Biol 115:49–58

Hadjantonakis AK, Macmaster S, Nagy A (2002) Embryonic stem cells and mice expressing different GFP variants for multiple non-invasive reporter usage within a single animal. BMC Biotechnol 2:11

Hagani AB RI, Tan C, Krause A, Sadelain M (1999) Activation conditions determine susceptibility of murine primary T-lymphocytes to retroviral infection. J Gene Med 1:341–351

Hain SF, Maisey MN (2003) Positron emission tomography for urological tumours. BJU Int 92:159–164

Halbhuber KJ, Konig K (2003) Modern laser scanning microscopy in biology, biotechnology and medicine. Ann Anat 185:1–20

Hardy J EM, Bachmann MH, Negrin RS, Fathman CG, Contag CH (2001) Bioluminescence imaging of lymphocyte trafficking in vivo. Exp Hematol 29:1353–1360

Harisinghani MG, Barentsz J, Hahn PF, Deserno WM, Tabatabaei S, van de Kaa CH, de la Rosette J, Weissleder R (2003) Noninvasive detection of clinically occult lymph-node metastases in prostate cancer. N Engl J Med 348:2491–2499

Harrington KJ, Linardakis E, Vile RG (2000) Transcriptional control: an essential component of cancer gene therapy strategies? Adv Drug Deliv Rev 44:167–184

Haubner R, Wester HJ, Weber WA, Mang C, Ziegler SI, Goodman SL, Senekowitsch-Schmidtke R, Kessler H, Schwaiger M (2001) Noninvasive imaging of alpha(v)beta3 integrin expression using 18F-labeled RGD-containing glycopeptide and positron emission tomography. Cancer Res 61:1781–1785

Hennig J, Speck O, Koch MA, Weiller C (2003) Functional magnetic resonance imaging: a review of methodological aspects and clinical applications. J Magn Reson Imaging 18:1–15

Hill JM, Dick AJ, Raman VK, Thompson RB, Yu ZX, Hinds KA, Pessanha BS, Guttman MA, Varney TR, Martin BJ, Dunbar CE, McVeigh ER, Lederman RJ (2003) Serial cardiac magnetic resonance imaging of injected mesenchymal stem cells. Circulation 108:1009–1014

Hinds KA, Hill JM, Shapiro EM, Laukkanen MO, Silva AC, Combs CA, Varney TR, Balaban RS, Koretsky AP, Dunbar CE (2003) Highly efficient endosomal labeling of progenitor and stem

cells with large magnetic particles allows magnetic resonance imaging of single cells. Blood 102:867–872

Hockel M, Schlenger K, Aral B, Mitze M, Schaffer U, Vaupel P (1996) Association between tumor hypoxia and malignant progression in advanced cancer of the uterine cervix. Cancer Res 56:4509–4515

Hoehn M, Kustermann E, Blunk J, Wiedermann D, Trapp T, Wecker S, Focking M, Arnold H, Hescheler J, Fleischmann BK, Schwindt W, Buhrle C (2002) Monitoring of implanted stem cell migration in vivo: a highly resolved in vivo magnetic resonance imaging investigation of experimental stroke in rat. Proc Natl Acad Sci U S A 99:16267–16272

Hoekstra CJ, Stroobants SG, Hoekstra OS, Vansteenkiste J, Biesma B, Schramel FJ, van Zandwijk N, van Tinteren H, Smit EF (2003) The value of [18F]fluoro-2-deoxy-D-glucose positron emission tomography in the selection of patients with stage IIIA-N2 non-small cell lung cancer for combined modality treatment. Lung Cancer 39:151–157

Hoffman RM (2005) The multiple uses of fluorescent proteins to visualize cancer in vivo. Nat Rev Cancer 5: 796–806

Holland E (2004a) Mouse models of human cancer. Wiley-Liss, New York

Holland EC (2004b) Mouse models of human cancer as tools in drug development. Cancer Cell 6:197–198

Ichikawa T, Hogemann D, Saeki Y, Tyminski E, Terada K, Weissleder R, Chiocca EA, Basilion JP (2002) MRI of transgene expression: correlation to therapeutic gene expression. Neoplasia 4:523–530

Iida H, Rhodes CG, Araujo LI, Yamamoto Y, de Silva R, Maseri A, Jones T (1996) Noninvasive quantification of regional myocardial metabolic rate for oxygen by use of 15O2 inhalation and positron emission tomography. Theory, error analysis, and application in humans. Circulation 94:792–807

Ivan M, Kondo K, Yang H, Kim W, Valiando J, Ohh M, Salic A, Asara JM, Lane WS, Kaelin WG, Jr. (2001) HIFalpha targeted for VHL-mediated destruction by proline hydroxylation: implications for O2 sensing. Science 292:464–468

Iyer M, Barrio JR, Namavari M, Bauer E, Satyamurthy N, Nguyen K, Toyokuni T, Phelps ME, Herschman HR, Gambhir SS (2001a) 8-[18F]Fluoropenciclovir: an improved reporter probe for imaging HSV1-tk reporter gene expression in vivo using PET. J Nucl Med 42:96–105

Iyer M, Wu L, Carey M, Wang Y, Smallwood A, Gambhir SS (2001b) Two-step transcriptional amplification as a method for imaging reporter gene expression using weak promoters. Proc Natl Acad Sci USA 98:14595–14600

Jacobs A, Tjuvajev JG, Dubrovin M, Akhurst T, Balatoni J, Beattie B, Joshi R, Finn R, Larson SM, Herrlinger U, Pechan PA, Chiocca EA, Breakefield XO, Blasberg RG (2001a) Positron emission tomography-based imaging of transgene expression mediated by replication-conditional, oncolytic herpes simplex virus type 1 mutant vectors in vivo. Cancer Res 61:2983–2995

Jacobs A, Voges J, Reszka R, Lercher M, Gossmann A, Kracht L, Kaestle C, Wagner R, Wienhard K, Heiss WD (2001b) Positron-emission tomography of vector-mediated gene expression in gene therapy for gliomas. Lancet 358:727–729

Jacobs RE AE, Meade TJ, Fraser SE (1999) Looking deeper into vertebrate development. Trends Cell Biol 9:73–76

Jaffer FA, Tung CH, Gerszten RE, Weissleder R (2002) In vivo imaging of thrombin activity in experimental thrombi with thrombin-sensitive near-infrared molecular probe. Arterioscler Thromb Vasc Biol 22:1929–1935

Johnson GA BH, Black RD, Hedlund LW, Maronpot RR, Smith BR (1993) Histology by magnetic resonance microscopy. Magn Reson Q 9:1–30

Kaelin WG Jr (2005) The von Hippel-Lindau protein, HIF hydroxylation, and oxygen sensing. Biochem Biophys Res Commun 338:627–638

Kelly RF, Tran T, Holmstrom A, Murar J, Segurola RJ, Jr. (2004) Accuracy and cost-effectiveness of [18F]-2-fluoro-deoxy-D-glucose-positron emission tomography scan in potentially resectable non-small cell lung cancer. Chest 125:1413–1423

Kiani A RA, Aramburu J (2000) Manipulating immune responses with immunosuppressive agents that target NFAT. Immunity 12:359–372

Kircher MF AJ, Graves EE, Love V, Josephson L, Lichtman AH, Weissleder R (2003) In vivo high resolution three-dimensional imaging of antigen-specific cytotoxic T-lymphocyte trafficking to tumors. Cancer Res 63:6838–6846

Koch CJ, Evans SM (2003) Non-invasive PET and SPECT imaging of tissue hypoxia using isotopically labeled 2-nitroimidazoles. Adv Exp Med Biol 510:285–292

Koehne G, Doubrovin, M, Doubrovina, E, Zanzonico, P, Gallardo, HF, Ivanova, A, Balatoni, J, Teruya-Feldstein, J, Heller, G, May, C, Ponomarev, V, Ruan, S, Finn, R, Blasberg, RG, Bornmann, W, Riviere, I, Sadelain, M, O'Reilly, RJ, Larson, SM, Gelovani Tjuvajev, JG. (2003) Serial in vivo imaging of the targeted migration of human HSV-TK-transduced antigen-specific lymphocytes. Nat Biotechnol 21:405–413

Kolb VA, Makeyev EV, Spirin AS (2000) Co-translational folding of an eukaryotic multidomain protein in a prokaryotic translation system. J Biol Chem 275:16597–16601

Korf J V-vdDL, Brinkman-Medema R, Niemarkt A, de Leij LF (1998) Divalent cobalt as a label to study lymphocyte distribution using PET and SPECT. J Nucl Med 39:836–841

Kostura L, Kraitchman DL, Mackay AM, Pittenger MF, Bulte JW (2004) Feridex labeling of mesenchymal stem cells inhibits chondrogenesis but not adipogenesis or osteogenesis. NMR Biomed 17:513–517

Krishna MC, Subramanian S, Kuppusamy P, Mitchell JB (2001) Magnetic resonance imaging for in vivo assessment of tissue oxygen concentration. Semin Radiat Oncol 11:58–69

Labas YA, Gurskaya NG, Yanushevich YG, Fradkov AF, Lukyanov KA, Lukyanov SA, Matz MV (2002) Diversity and evolution of the green fluorescent protein family. Proc Natl Acad Sci USA 99:4256–4261

Lalwani AK, Han JJ, Walsh BJ, Zolotukhin S, Muzyczka N, Mhatre AN (1997) Green fluorescent protein as a reporter for gene transfer studies in the cochlea. Hear Res 114:139–147

Larson SM, Morris M, Gunther I, Beattie B, Humm JL, Akhurst TA, Finn RD, Erdi Y, Pentlow K, Dyke J, Squire O, Bornmann W, McCarthy T, Welch M, Scher H (2004) Tumor localization of 16beta-18F-fluoro-5alpha-dihydrotestosterone versus 18F-FDG in patients with progressive, metastatic prostate cancer. J Nucl Med 45:366–373

Laxman B, Hall DE, Bhojani MS, Hamstra DA, Chenevert TL, Ross BD, Rehemtulla A (2002) Noninvasive real-time imaging of apoptosis. Proc Natl Acad Sci USA 99:16551–16555

Lazar-Molnar E, Hegyesi H, Toth S, Falus A (2000) Autocrine and paracrine regulation by cytokines and growth factors in melanoma. Cytokine 12:547–554

Lee KH, Kim HK, Paik JY, Matsui T, Choe YS, Choi Y, Kim BT (2005) Accuracy of myocardial sodium/iodide symporter gene expression imaging with radioiodide: evaluation with a dual-gene adenovirus vector. J Nucl Med 46:652–657

Lehtio K, Eskola O, Viljanen T, Oikonen V, Gronroos T, Sillanmaki L, Grenman R, Minn H (2004) Imaging perfusion and hypoxia with PET to predict radiotherapy response in head-and-neck cancer. Int J Radiat Oncol Biol Phys 59:971–982

Levy JP, Muldoon RR, Zolotukhin S, Link CJ, Jr. (1996) Retroviral transfer and expression of a humanized, red-shifted green fluorescent protein gene into human tumor cells. Nat Biotechnol 14:610–614

Lewin M, Carlesso N, Tung CH, Tang XW, Cory D, Scadden DT, Weissleder R (2000) Tat peptide-derivatized magnetic nanoparticles allow in vivo tracking and recovery of progenitor cells. Nat Biotechnol 18 410–414

Lewis JS, Welch MJ (2001) PET imaging of hypoxia. Q J Nucl Med 45:183–188

Li W HR (1996) Regulation of the nuclear factor of activated T cells in stably transfected Jurkat cell clones. Biochem Biophys Res Commun 219:96–99

Liang Q, Satyamurthy N, Barrio JR, Toyokuni T, Phelps MP, Gambhir SS, Herschman HR (2001) Noninvasive, quantitative imaging in living animals of a mutant dopamine D2 receptor reporter gene in which ligand binding is uncoupled from signal transduction. Gene Ther 8:1490–1498

Loncaster JA, Harris AL, Davidson SE, Logue JP, Hunter RD, Wycoff CC, Pastorek J, Ratcliffe PJ, Stratford IJ, West CM (2001) Carbonic anhydrase (CA IX) expression, a potential new intrinsic

marker of hypoxia: correlations with tumor oxygen measurements and prognosis in locally advanced carcinoma of the cervix. Cancer Res 61:6394–6399

Louie AY, Huber MM, Ahrens ET, Rothbacher U, Moats R, Jacobs RE, Fraser SE, Meade TJ (2000) In vivo visualization of gene expression using magnetic resonance imaging. Nat Biotechnol 18:321–325

Luker GD, Sharma V, Pica CM, Dahlheimer JL, Li W, Ochesky J, Ryan CE, Piwnica-Worms H, Piwnica-Worms D (2002) Noninvasive imaging of protein-protein interactions in living animals. Proc Natl Acad Sci USA 99:6961–6966

Luker GD, Pica CM, Song J, Luker KE, Piwnica-Worms D (2003a) Imaging 26S proteasome activity and inhibition in living mice. Nat Med 9:969–973

Luker GD, Sharma V, Pica CM, Prior JL, Li W, Piwnica-Worms D (2003b) Molecular imaging of protein-protein interactions: controlled expression of p53 and large T-antigen fusion proteins in vivo. Cancer Res 63:1780–1788

Luker GD, Sharma V, Piwnica-Worms D (2003c) Visualizing protein-protein interactions in living animals. Methods 29:110–122

Lynch TJ, Bell DW, Sordella R, Gurubhagavatula S, Okimoto RA, Brannigan BW, Harris PL, Haserlat SM, Supko JG, Haluska FG, Louis DN, Christiani DC, Settleman J, Haber DA (2004) Activating mutations in the epidermal growth factor receptor underlying responsiveness of non-small-cell lung cancer to gefitinib. N Engl J Med 350:2129–2139

Lyons SK, Meuwissen R, Krimpenfort P, Berns A (2003) The generation of a conditional reporter that enables bioluminescence imaging of Cre/loxP-dependent tumorigenesis in mice. Cancer Res 63:7042–7046

Lyons SK, Lim E, Clermont AO, Dusich J, Zhu L, Campbell KD, Coffee RJ, Grass DS, Hunter J, Purchio T, Jenkins D (2006) Noninvasive bioluminescence imaging of normal and spontaneously transformed prostate tissue in mice. Cancer Res 66:4701–4707

Maschauer S, Prante O, Hoffmann M, Deichen JT, Kuwert T (2004) Characterization of 18F-FDG uptake in human endothelial cells in vitro. J Nucl Med 45:455–460

Mathieu S, El-Battari A (2003) Monitoring E-selectin-mediated adhesion using green and red fluorescent proteins. J Immunol Methods 272:81–92

Matz MV, Fradkov AF, Labas YA, Savitsky AP, Zaraisky AG, Markelov ML, Lukyanov SA (1999) Fluorescent proteins from nonbioluminescent Anthozoa species. Nat Biotechnol 17:969–973

Mayer-Kuckuk P, Banerjee D, Malhotra S, Doubrovin M, Iwamoto M, Akhurst T, Balatoni J, Bornmann W, Finn R, Larson S, Fong Y, Gelovani Tjuvajev J, Blasberg R, Bertino JR (2002) Cells exposed to antifolates show increased cellular levels of proteins fused to dihydrofolate reductase: a method to modulate gene expression. Proc Natl Acad Sci USA 99:3400–3405

Mayer-Kuckuk P, Menon LG, Blasberg RG, Bertino JR, Banerjee D (2004) Role of reporter gene imaging in molecular and cellular biology. Biol Chem 385:353–361

Mayer-Kuckuk P, Doubrovin M, Bidaut L, Budak-Alpdogan T, Cai S, Hubbard V, Alpdogan O, van den Brink M, Bertino JR, Blasberg RG, Banerjee D, Gelovani J (2006) Molecular imaging reveals skeletal engraftment sites of transplanted bone marrow cells. Cell Transplant 15:75–82

Min JJ, Gambhir SS (2004) Gene therapy progress and prospects: noninvasive imaging of gene therapy in living subjects. Gene Ther 11:115–125

Min JJ, Iyer M, Gambhir SS (2003) Comparison of [18F]FHBG and [14C]FIAU for imaging of HSV1-tk reporter gene expression: adenoviral infection vs stable transfection. Eur J Nucl Med Mol Imaging 30:1547–1560

Moberg KH, Logan TJ, Tyndall WA, Hall DJ (1992) Three distinct elements within the murine c-myc promoter are required for transcription. Oncogene 7:411–421

Myers WG (1979) Georg Charles de Hevesy: the father of nuclear medicine. J Nucl Med 20: 590–594

Nakagawa S, Massie B, Hawley RG (2001) Tetracycline-regulatable adenovirus vectors: pharmacologic properties and clinical potential. Eur J Pharm Sci 13:53–60

Neckers L (2002) Hsp90 inhibitors as novel cancer chemotherapeutic agents. Trends Mol Med 8:S55–S61

Neumaier M, Shively L, Chen FS, Gaida FJ, Ilgen C, Paxton RJ, Shively JE, Riggs AD (1990) Cloning of the genes for T84.66, an antibody that has a high specificity and affinity for carcinoembryonic antigen, and expression of chimeric human/mouse T84.66 genes in myeloma and Chinese hamster ovary cells. Cancer Res 50:2128–2134

Nordsmark M, Overgaard M, Overgaard J (1996) Pretreatment oxygenation predicts radiation response in advanced squamous cell carcinoma of the head and neck. Radiother Oncol 41:31–39

Nordsmark M, Loncaster J, Aquino-Parsons C, Chou SC, Ladekarl M, Havsteen H, Lindegaard JC, Davidson SE, Varia M, West C, Hunter R, Overgaard J, Raleigh JA (2003) Measurements of hypoxia using pimonidazole and polarographic oxygen-sensitive electrodes in human cervix carcinomas. Radiother Oncol 67:35–44

Olafsen T, Kenanova VE, Sundaresan G, Anderson AL, Crow D, Yazaki PJ, Li L, Press MF, Gambhir SS, Williams LE, Wong JY, Raubitschek AA, Shively JE, Wu AM (2005) Optimizing radiolabeled engineered anti-p185HER2 antibody fragments for in vivo imaging. Cancer Res 65:5907–5916

Olasz EB, Lang L, Seidel J, Green MV, Eckelman WC, Katz SI (2002) Fluorine-18 labeled mouse bone marrow-derived dendritic cells can be detected in vivo by high resolution projection imaging. J Immunol Methods 260:137–148

Oliver RJ, Woodwards RT, Sloan P, Thakker NS, Stratford IJ, Airley RE (2004) Prognostic value of facilitative glucose transporter Glut-1 in oral squamous cell carcinomas treated by surgical resection; results of EORTC Translational Research Fund studies. Eur J Cancer 40:503–507

Oswald F, Lovec H, Moroy T, Lipp M (1994) E2F-dependent regulation of human MYC: transactivation by cyclins D1 and A overrides tumour suppressor protein functions. Oncogene 9:2029–2036

Overbeek PA, Chepelinsky AB, Khillan JS, Piatigorsky J, Westphal H (1985) Lens-specific expression and developmental regulation of the bacterial chloramphenicol acetyltransferase gene driven by the murine alpha A-crystallin promoter in transgenic mice. Proc Natl Acad Sci USA 82:7815–7819

Palm S, Enmon RM, Jr., Matei C, Kolbert KS, Xu S, Zanzonico PB, Finn RL, Koutcher JA, Larson SM, Sgouros G (2003) Pharmacokinetics and Biodistribution of (86)Y-Trastuzumab for (90)Y dosimetry in an ovarian carcinoma model: correlative MicroPET and MRI. J Nucl Med 44:1148–1155

Papadakis ED, Nicklin SA, Baker AH, White SJ (2004) Promoters and control elements: designing expression cassettes for gene therapy. Curr Gene Ther 4:89–113

Papierniak CK BR, Kretschmer RR, Gotoff SP, Colombetti LG (1976) Technetium-99m labeling of human monocytes for chemotactic studies. J Nucl Med 17:988–992

Peng T, Golub TR, Sabatini DM (2002) The immunosuppressant rapamycin mimics a starvation-like signal distinct from amino acid and glucose deprivation. Mol Cell Biol 22:5575–5584

Penuelas I, Mazzolini G, Boan JF, Sangro B, Marti-Climent J, Ruiz M, Ruiz J, Satyamurthy N, Qian C, Barrio JR, Phelps ME, Richter JA, Gambhir SS, Prieto J (2005) Positron emission tomography imaging of adenoviral-mediated transgene expression in liver cancer patients. Gastroenterology 128:1787–1795

Phillips JA, Craig SJ, Bayley D, Christian RA, Geary R, Nicklin PL (1997) Pharmacokinetics, metabolism, and elimination of a 20-mer phosphorothioate oligodeoxynucleotide (CGP 69846A) after intravenous and subcutaneous administration. Biochem Pharmacol 54:657–668

Pichler A, Prior JL, Piwnica-Worms D (2004) Imaging reversal of multidrug resistance in living mice with bioluminescence: MDR1 P-glycoprotein transports coelenterazine. Proc Natl Acad Sci USA 101:1702–1707

Ponomarev V, Doubrovin M, Lyddane C, Beresten T, Balatoni J, Bornman W, Finn R, Akhurst T, Larson S, Blasberg R, Sadelain M, Tjuvajev JG (2001) Imaging TCR-dependent NFAT-mediated T-cell activation with positron emission tomography in vivo. Neoplasia 3:480–488

Ponomarev V, Doubrovin M, Serganova I, Beresten T, Vider J, Shavrin A, Ageyeva L, Balatoni J, Blasberg R, Tjuvajev JG (2003) Cytoplasmically retargeted HSV1-tk/GFP reporter gene mutants for optimization of noninvasive molecular-genetic imaging. Neoplasia 5:245–254

Ponomarev V, Doubrovin M, Serganova I, Vider J, Shavrin A, Beresten T, Ivanova A, Ageyeva L, Tourkova V, Balatoni J, Bornmann W, Blasberg R, Gelovani Tjuvajev J (2004) A novel triple-modality reporter gene for whole-body fluorescent, bioluminescent, and nuclear noninvasive imaging. Eur J Nucl Med Mol Imaging 31:740–751

Qiao J, Doubrovin M, Sauter BV, Huang Y, Guo ZS, Balatoni J, Akhurst T, Blasberg RG, Tjuvajev JG, Chen SH, Woo SL (2002) Tumor-specific transcriptional targeting of suicide gene therapy. Gene Ther 9: 168–175

Rannie GH TM, Ford WL (1977) An experimental comparison of radioactive labels with potential application to lymphocyte migration studies in patients. Clin Exp Immunol 29: 509–514

Rasey JS, Koh WJ, Evans ML, Peterson LM, Lewellen TK, Graham MM, Krohn KA (1996) Quantifying regional hypoxia in human tumors with positron emission tomography of [18F]fluoromisonidazole: a pretherapy study of 37 patients. Int J Radiat Oncol Biol Phys 36:417–428

Ray P, Bauer E, Iyer M, Barrio JR, Satyamurthy N, Phelps ME, Herschman HR, Gambhir SS (2001) Monitoring gene therapy with reporter gene imaging. Semin Nucl Med 31:312–320

Ray P, Pimenta H, Paulmurugan R, Berger F, Phelps ME, Iyer M, Gambhir SS (2002) Noninvasive quantitative imaging of protein-protein interactions in living subjects. Proc Natl Acad Sci USA 99:3105–3110

Ray P, Wu AM, Gambhir SS (2003) Optical bioluminescence and positron emission tomography imaging of a novel fusion reporter gene in tumor xenografts of living mice. Cancer Res 63:1160–1165

Ray S, Paulmurugan R, Hildebrandt I, Iyer M, Wu L, Carey M, Gambhir SS (2004) Novel bidirectional vector strategy for amplification of therapeutic and reporter gene expression. Hum Gene Ther 15:681–690

Rehemtulla A, Stegman LD, Cardozo SJ, Gupta S, Hall DE, Contag CH, Ross BD (2000) Rapid and quantitative assessment of cancer treatment response using in vivo bioluminescence imaging. Neoplasia 2:491–495

Rogers BE, Zinn KR, Buchsbaum DJ (2000) Gene transfer strategies for improving radiolabeled peptide imaging and therapy. Q J Nucl Med 44:208–223

Sadeghi H, Hitt MM (2005) Transcriptionally targeted adenovirus vectors. Curr Gene Ther 5: 411–427

Salceda S, Caro J (1997) Hypoxia-inducible factor 1alpha (HIF-1alpha) protein is rapidly degraded by the ubiquitin-proteasome system under normoxic conditions. Its stabilization by hypoxia depends on redox-induced changes. J Biol Chem 272:22642–22647

Schelling M, Avril N, Nahrig J, Kuhn W, Romer W, Sattler D, Werner M, Dose J, Janicke F, Graeff H, Schwaiger M (2000) Positron emission tomography using [(18)F]Fluorodeoxyglucose for monitoring primary chemotherapy in breast cancer. J Clin Oncol 18:1689–1695

Serganova I, Doubrovin M, Vider J, Ponomarev V, Soghomonyan S, Beresten T, Ageyeva L, Serganov A, Cai S, Balatoni J, Blasberg R, Gelovani J (2004) Molecular imaging of temporal dynamics and spatial heterogeneity of hypoxia-inducible factor-1 signal transduction activity in tumors in living mice. Cancer Res 64:6101–6108

Shah K, Jacobs A, Breakefield XO, Weissleder R (2004) Molecular imaging of gene therapy for cancer. Gene Ther 11:1175–1187

Shaner NC, Steinbach PA, Tsien RY (2005) A guide to choosing fluorescent proteins. Nat Methods 2:905–909

Shaner NC, Campbell RE, Steinbach PA, Giepmans BN, Palmer AE, Tsien RY (2004) Improved monomeric red, orange and yellow fluorescent proteins derived from Discosoma sp. red fluorescent protein. Nat Biotechnol 22:1567–1572

Sherr CJ, McCormick F (2002) The RB and p53 pathways in cancer. Cancer Cell 2:103–112

Shin JH, Chung JK, Kang JH, Lee YJ, Kim KI, So Y, Jeong JM, Lee DS, Lee MC (2004) Noninvasive imaging for monitoring of viable cancer cells using a dual-imaging reporter gene. J Nucl Med 45:2109–2115

Shreve PD, Anzai Y, Wahl RL (1999) Pitfalls in oncologic diagnosis with FDG PET imaging: physiologic and benign variants. Radiographics 19:61–77; quiz 150–151

Smith-Jones PM, Solit DB, Akhurst T, Afroze F, Rosen N, Larson SM (2004) Imaging the pharmacodynamics of HER2 degradation in response to Hsp90 inhibitors. Nat Biotechnol 22:701–706

Stamm C, Westphal B, Kleine HD, Petzsch M, Kittner C, Klinge H, Schumichen C, Nienaber CA, Freund M, Steinhoff G (2003) Autologous bone-marrow stem-cell transplantation for myocardial regeneration. Lancet 361:45–46

Su H FA, Gambhir SS, Braun J (2004) Quantitation of cell number by a positron emission tomography reporter gene strategy. Mol Imaging Biol 6:139–148

Sundaresan G, Yazaki PJ, Shively JE, Finn RD, Larson SM, Raubitschek AA, Williams LE, Chatzioannou AF, Gambhir SS, Wu AM (2003) 124I-labeled engineered anti-CEA minibodies and diabodies allow high-contrast, antigen-specific small-animal PET imaging of xenografts in athymic mice. J Nucl Med 44:1962–1969

Tavitian B (2000) In vivo antisense imaging. Q J Nucl Med 44:236–255

Tavitian B, Terrazzino S, Kuhnast B, Marzabal S, Stettler O, Dolle F, Deverre JR, Jobert A, Hinnen F, Bendriem B, Crouzel C, Di Giamberardino L (1998) In vivo imaging of oligonucleotides with positron emission tomography. Nat Med 4:467–471

Thomas GV, Tran C, Mellinghoff IK, Welsbie DS, Chan E, Fueger B, Czernin J, Sawyers CL (2006) Hypoxia-inducible factor determines sensitivity to inhibitors of mTOR in kidney cancer. Nat Med 12:122–127

Thompson JF, Hayes LS, Lloyd DB (1991) Modulation of firefly luciferase stability and impact on studies of gene regulation. Gene 103:171–177

Tjuvajev J, Gansbacher B, Desai R, Beattie B, Kaplitt M, Matei C, Koutcher J, Gilboa E, Blasberg R (1995a) RG-2 glioma growth attenuation and severe brain edema caused by local production of interleukin-2 and interferon-gamma. Cancer Res 55:1902–1910

Tjuvajev JG, Stockhammer G, Desai R, Uehara H, Watanabe K, Gansbacher B, Blasberg RG (1995b) Imaging the expression of transfected genes in vivo. Cancer Res 55:6126–6132

Tjuvajev JG, Finn R, Watanabe K, Joshi R, Oku T, Kennedy J, Beattie B, Koutcher J, Larson S, Blasberg RG (1996) Noninvasive imaging of herpes virus thymidine kinase gene transfer and expression: a potential method for monitoring clinical gene therapy. Cancer Res 56:4087–4095

Tjuvajev JG, Avril N, Oku T, Sasajima T, Miyagawa T, Joshi R, Safer M, Beattie B, DiResta G, Daghighian F, Augensen F, Koutcher J, Zweit J, Humm J, Larson SM, Finn R, Blasberg R (1998) Imaging herpes virus thymidine kinase gene transfer and expression by positron emission tomography. Cancer Res 58:4333–4341

Tjuvajev JG, Chen SH, Joshi A, Joshi R, Guo ZS, Balatoni J, Ballon D, Koutcher J, Finn R, Woo SL, Blasberg RG (1999) Imaging adenoviral-mediated herpes virus thymidine kinase gene transfer and expression in vivo. Cancer Res 59:5186–5193

Tjuvajev J, Blasberg R, Luo X, Zheng LM, King I, Bermudes D (2001) Salmonella-based tumor-targeted cancer therapy: tumor amplified protein expression therapy (TAPET) for diagnostic imaging. J Control Release 74:313–315

Tjuvajev JG, Doubrovin M, Akhurst T, Cai S, Balatoni J, Alauddin MM, Finn R, Bornmann W, Thaler H, Conti PS, Blasberg RG (2002) Comparison of radiolabeled nucleoside probes (FIAU, FHBG, and FHPG) for PET imaging of HSV1-tk gene expression. J Nucl Med 43:1072–1083

Tomita S, Mickle DA, Weisel RD, Jia ZQ, Tumiati LC, Allidina Y, Liu P, Li RK (2002) Improved heart function with myogenesis and angiogenesis after autologous porcine bone marrow stromal cell transplantation. J Thorac Cardiovasc Surg 123:1132–1140

Tuveson DA, Willis NA, Jacks T, Griffin JD, Singer S, Fletcher CD, Fletcher JA, Demetri GD (2001) STI571 inactivation of the gastrointestinal stromal tumor c-KIT oncoprotein: biological and clinical implications. Oncogene 20:5054–5058

Uhrbom L, Nerio E, Holland EC (2004) Dissecting tumor maintenance requirements using bioluminescence imaging of cell proliferation in a mouse glioma model. Nat Med 10:1257–1260

van den Abbeele A (2001) F18-FDG-PET provides early evidence of biological response to ST1571 pateins with malignant gastointestinal stromal tumors (GIST). Proc Am Soc Clin Oncol 20:362a

Vose JM, Bierman PJ, Anderson JR, Harrison KA, Dalrymple GV, Byar K, Kessinger A, Armitage JO (1996) Single-photon emission computed tomography gallium imaging versus

computed tomography: predictive value in patients undergoing high-dose chemotherapy and autologous stem-cell transplantation for non-Hodgkin's lymphoma. J Clin Oncol 14:2473–2479
Wang GL, Semenza GL (1995) Purification and characterization of hypoxia-inducible factor 1. J Biol Chem 270:1230–1237
Wang L, Jackson WC, Steinbach PA, Tsien RY (2004) Evolution of new nonantibody proteins via iterative somatic hypermutation. Proc Natl Acad Sci USA 101:16745–16749
Wang X, Rosol M, Ge S, Peterson D, McNamara G, Pollack H, Kohn DB, Nelson MD, Crooks GM (2003) Dynamic tracking of human hematopoietic stem cell engraftment using in vivo bioluminescence imaging. Blood 102:3478–3482
Wang Y, Iyer M, Annala A, Wu L, Carey M, Gambhir SS (2006) Noninvasive indirect imaging of vascular endothelial growth factor gene expression using bioluminescence imaging in living transgenic mice. Physiol Genomics 24:173–180
Warburg O (1956) On the origin of cancer cells. Science 123:309–314
Weber WA, Petersen V, Schmidt B, Tyndale-Hines L, Link T, Peschel C, Schwaiger M (2003) Positron emission tomography in non-small-cell lung cancer: prediction of response to chemotherapy by quantitative assessment of glucose use. J Clin Oncol 21:2651–2657
Weissleder R (2002) Scaling down imaging: molecular mapping of cancer in mice. Nat Rev Cancer 2:11–18
Weissleder R, Ntziachristos V (2003) Shedding light onto live molecular targets. Nat Med 9: 123–128
Weissleder R, Simonova M, Bogdanova A, Bredow S, Enochs WS, Bogdanov A Jr (1997) MR imaging and scintigraphy of gene expression through melanin induction. Radiology 204: 425–429
Wilson T, Hastings JW (1998) Bioluminescence. Annu Rev Cell Dev Biol 14:197–230
Wong KK, Zou X, Merrell KT, Patel AJ, Marcu KB, Chellappan S, Calame K (1995) v-Abl activates c-myc transcription through the E2F site. Mol Cell Biol 15:6535–6544
Wu AM (2004) Engineering multivalent antibody fragments for in vivo targeting. Methods Mol Biol 248:209–225
Wu AM, Senter PD (2005) Arming antibodies: prospects and challenges for immunoconjugates. Nat Biotechnol 23:1137–1146
Wu JC, Inubushi M, Sundaresan G, Schelbert HR, Gambhir SS (2002) Optical imaging of cardiac reporter gene expression in living rats. Circulation 105:1631–1634
Yaghoubi S, Barrio JR, Dahlbom M, Iyer M, Namavari M, Satyamurthy N, Goldman R, Herschman HR, Phelps ME, Gambhir SS (2001) Human pharmacokinetic and dosimetry studies of [(18)F]FHBG: a reporter probe for imaging herpes simplex virus type-1 thymidine kinase reporter gene expression. J Nucl Med 42:1225–1234
Yaghoubi SS, Barrio JR, Namavari M, Satyamurthy N, Phelps ME, Herschman HR, Gambhir SS (2005) Imaging progress of herpes simplex virus type 1 thymidine kinase suicide gene therapy in living subjects with positron emission tomography. Cancer Gene Ther 12:329–339
Yu YA, Timiryasova T, Zhang Q, Beltz R, Szalay AA (2003) Optical imaging: bacteria, viruses, and mammalian cells encoding light-emitting proteins reveal the locations of primary tumors and metastases in animals. Anal Bioanal Chem 377:964–972
Zhang L, Adams JY, Billick E, Ilagan R, Iyer M, Le K, Smallwood A, Gambhir SS, Carey M, Wu L (2002) Molecular engineering of a two-step transcription amplification (TSTA) system for transgene delivery in prostate cancer. Mol Ther 5:223–232
Zhang W FJ, Harris SE, Contag PR, Stevenson DK, Contag CH (2001) Rapid in vivo functional analysis of transgenes in mice using whole body imaging of luciferase expression. Transgenic Res 10:423-434
Zhu ZB, Makhija SK, Lu B, Wang M, Kaliberova L, Liu B, Rivera AA, Nettelbeck DM, Mahasreshti PJ, Leath CA, 3rd, Yamamoto M, Alvarez RD, Curiel DT (2004) Transcriptional targeting of adenoviral vector through the CXCR4 tumor-specific promoter. Gene Ther 11: 645–648